PRODUCTION AND SEPARATION OF GLUCOSE FROM CELLULOSE HYDROLYSATES USING MEMBRANE REACTOR: EFFECT OF TRANSMEMBRANE PRESSURE AND CROSS FLOW VELOCITY

MOHD HAFIZUDDIN BIN ZAHARI

UNIVERSITI MALAYSIA PAHANG

PRODUCTION AND SEPARATION OF GLUCOSE FROM CELLULOSE HYDROLYSATES USING MEMBRANE REACTOR: EFFECT OF TRANSMEMBRANE PRESSURE AND CROSS FLOW VELOCITY

MOHD HAFIZUDDIN BIN ZAHARI

A thesis submitted in fulfillment
of the requirements for the award of the degree of
Bachelor of Chemical Engineering (Biotechnology)

Faculty of Chemical & Natural Resources Engineering
Universiti Malaysia Pahang

JANUARY 2012

SUPERVISOR'S DECLARATION

I hereby declare that I have read this thesis and in my opinion, this thesis is adequate in terms of scope and quality for the award of the degree of Bachelor of Chemical Engineering (Biotechnology).

Signature   :   ……………………………….

Name of Supervisor   :   Assoc. Prof. Dr. Mimi Sakinah Bt. Abd Munaim

Date   :   26 January 2012

STUDENT'S DECLARATION

I hereby declare that the work in this thesis entitled "Production and separation of glucose from cellulose hydrolysates using membrane reactor: Effect of transmembrane pressure and cross flow velocity" is my own research except as cited in references. The thesis has not been accepted for any degree and is not concurrently submitted for award of other degree.

Signature   :   ………………………..

Name   :   Mohd Hafizuddin Bin Zahari

Date   :   26 January 2011

Dedicated to my

beloved father and mother,

loving brothers and sisters.

For their loves, supports and best wishes.

ACKNOWLEDGEMENTS

First and foremost, I am grateful toward ALLAH the almighty for the blessing given to me and for those I love, without which this project would has not been finished.

I would like to take this opportunity to express my sincere thanks and appreciation to my supervisor, Assoc. Prof. Dr. Mimi Sakinah Bt. Abd Munaim for her guidance, inspiration, patient, encouragement, critics and support in completing my final year project. The publication of this study would not be possible without her advice and encouragement. All lessons, advise and unparalleled knowledge shared would not be forgotten.

I am very thankful to Universiti Malaysia Pahang (UMP) for providing good facilities in the campus. Thanks to all the technical staff at Faculty of Chemical & Natural Resources Engineering, UMP.

Exclusive thanks to my family, for their support, encourage and patient throughout my final year project. I am very grateful to have family members that very supportive and understanding especially my mother and my beloved father. Thank you so much. To all my colleagues and friends, thanks for the support and the knowledge we had shared together.

ABSTRACT

Sawdust from hardwood contain large amount of cellulose and hemicellulose. Enzymatic hydrolysis of cellulose has larger potential in fulfil global food and energy demand by reducing sugar production such as glucose. In this study, the effect of transmembrane pressure (TMP) and cross-flow velocity (CFV) on permeate flux during the recovery and separation of glucose from cellulose hydrolysates by using membrane reactor was investigated. Two-stage pretreatment will be performed by using dilute sodium hydroxide (NaOH) and follow by dilute sulfuric acid (H_2SO_4) for about 24 hours at 75ºC respectively. Then, continued with enzymatic hydrolysis of cellulose with cellulase and cellobiase for 48 hours at 50 ºC and 150 rpm. Separation of glucose from cellulose hydrolysate will be performed by using ultrafiltration membrane for 60 minutes at 50ºC respectively. Then filtration method using ultrafiltration membrane was employed as a function of transmembrane pressure (TMP) and cross flow velocity (CFV), in order to identify their effects on the membrane flux and subsequently determine its optimum condition using response surface methodology (RSM). Filtration process was conducted at five different values of TMP and CFV range from 1 to 3 bars and 0.06 to 0.22 m/s respectively. The membrane flux after optimization was 116.655 L/m^2.h. The optimum conditions at TMP and CFV were found at 1 bar and 0.18 m/s.

ABSTRAK

Habuk kayu daripada kayu keras mengandungi sejumlah besar selulosa dan hemiselulosa. Hidrolisis enzim selulosa mempunyai potensi yang lebih besar dalam memenuhi makanan global dan permintaan tenaga dengan menghasilkan gula penurun seperti glukosa. Dalam kajian ini, kesan tekanan transmembran (TMP) dan halaju aliran silang (CFV) terhadap fluks semasa pemulihan dan pengasingan glukosa daripada hidrolisat selulosa dengan menggunakan reaktor membran telah dikaji. Dua peringkat pra-rawatan telah dilakukan dengan menggunakan natrium hidroksida cair (NaOH) dan diikuti dengan pra-rawatan menggunakan asid sulfurik (H_2SO_4) selama 24 jam pada suhu 75ºC. Kemudian, selulosa dihidrolisis oleh enzim selulase dan selubiase selama 48 jam pada 50ºC dan 150 rpm. Pengasingan glukosa daripada hidrolisat selulosa dilakukan menggunakan penapis ultra membran selama 60 minit pada 50ºC. Kesan tekanan transmembran (TMP) dan halaju aliran silang (CFV) terhadap fluks dikaji dan ditentukan keadaan optimumnya menggunakan kaedah tindakbalas permukaan (RSM). Proses penapisan telah dijalankan pada lima nilai TMP dan CFV yang berbeza dalam linkungan 1 hingga 3 bar dan 0.06 hingga 0.22 m/s. Nilai fluks maksimum terhasil adalah sebanyak 116.655 L/m^2.h. Keadaan optimum bagi kesan tekanan transmembran (TMP) dan halaju aliran silang (CFV) adalah pada 1 bar dan 0.18 m/s.

TABLE OF CONTENT

LIST OF TABLES

LIST OF FIGURES

LIST OF SYMBOLS

α	Alpha
β	Beta
°C	Degree C
C	Carbon
cm	Centimetre
g	Gram
J	Flux
kDa	Kilo Dalton
kg	Kilogram
L	Liter
$L/m^2.h$	Liter per meter square per hour
m	Meter
M	Molarity
ml	Millilitre
%	Percentage

LIST OF ABBREVIATIONS

Adj R^2	Adjusted R^2
ANOVA	Analysis of variance
CCD	Central composite design
CFV	Cross flow velocity
DNS	Dinitrosalicylic
DOE	Design of experiment
Et al	An others
FTIR	Fourier Transform Infrared
HCl	Hydrochloric acid
H$_2$SO$_4$	Sulphuric acid
NaOH	Sodium hydroxide
OFAT	One factor at a time
pH	Potentiometric hydrogen ion concentration
Q	Permeate flow rate in liter per minute
rpm	Rotary per minute
RSM	Response surface methodology
SEM	Scanning electron microscopy
TMP	Transmembrane pressure
MWCO	Molecular weight cut off

CHAPTER 1

INTRODUCTION

1.1   BACKGROUND OF STUDY

Logging activities in Malaysia was one of important economic activity, however the sodas generated from processing the wood was wasted. The sawdust could be used to extract reducing sugar by using membrane reactor. Enzymatic hydrolysis of cellulose to produce reducing sugar such as glucose has larger potential in fulfill global food and energy demand. Cellobiose obtained by enzymatic hydrolysis of cellulose and cellulose rich materials such as sawdust (meranti). Glucose is separated by membrane reactor from enzyme cellulase and cellobiase.

Lignocelluloses biomass primarily consists of cellulose, hemicelluloses, and lignin which are usually being used as raw materials in the production of ethanol. Lignocelluloses biomass is believed to be less expensive and more plentiful than either starch or sucrose containing feedstock. Forest residues such as sawdust and wood bark are believed to be one of the most abundant sources of sugars, although much research has been reported on herbaceous grass such as switch grass, agricultural residue such as corn stover and municipal waste (Hu *et al*., 2008).

Besides that, the polysaccharides namely; cellulose and hemicelluloses present in the lignocelluloses biomass need to be hydrolyzed with acids or enzymes in order to produce fermentable sugars. Pretreatment is an important tool for practical cellulose conversion processes. Pretreatment is required to alter the structure of cellulosic biomass to make cellulose more accessible to the enzymes that convert the carbohydrate polymers into fermentable sugars. Several studies have shown the potential of sodium

hydroxide pretreatment on a variety of lignocellulosic materials. Sodium hydroxide pretreatment can enhances lignocelluloses digestibility by increasing internal surface area, decreasing the degree of polymerization and the crystallinity of celluloses, and separating structural linkages between lignin and carbohydrates effectively which will decreased lignin content (Wang *et al.*, 2010).Apart from that, dilute acid pretreatment has been widely investigated due to its effectiveness and inexpensive method of pretreatment compared to other pretreatment methods. The dilute sulfuric acid pretreatment can effectively solubilized hemicelluloses into monomeric sugars and soluble oligomers, thus improving cellulose conversion (Sun and Cheng, 2005). Thus, the combination of this two pretreatment to recovery of celluloses from different biomasses especially from wood will be one of the most interesting industrial processes in the near future.

In biotechnology industries, membrane application is gradually emerge as a powerful bioseparation for purification, fractionation, separation and concentration of bioproducts (Sakinah *et al.*, 2008). Pressure driven membrane filtration, one of membrane separation processes has been used to separate and concentrate the hemicelluloses extracted from wood (Mohammad, 2008). This procedure could be used for the cellulose separation. Membrane processes are generally classified into different categories which ranging from reverse osmosis and nanofiltration to ultrafiltration and cross-flow microfiltration that could be used to separate the cellulose.

1.2   PROBLEM STATEMENT

Membrane fouling is one of the problems that limit the use of membrane separation due to slowdown the reaction and lead to filtration resistance. Thus, decrease the efficiency to separate glucose from cellulose hydrolysates. Membrane filter cannot be recycle and need to change because of fouling problems. Hence it will increase the operational cost. Other than that, enzyme used in enzymatic reaction cannot be recycled if the reaction process did not take place in membrane reactor.

1.3 OBJECTIVES

The objective of this study is to retain enzyme cellulase and separate glucose from cellulose hydrolysate using membrane reactor. The study will be specified on the effect of transmembrane pressure and cross flow velocity based on:

- Effect of transmembrane pressure for glucose separation from reaction mixture.

- Effect of cross flow velocity for glucose separation from reaction mixture.

- To optimize and determine optimum condition for separation of glucose from reaction mixture.

1.4 SCOPE OF STUDY

In order to achieve the objective of the research, the optimum operating parameters; and flux during separation process will be observed. The optimum operating conditions are transmembrane pressure (TMP) and cross flow velocity (CFV) is important to obtain the high flux of cellulose recovery with less possibility of membrane fouling. The separation process is performing at transmembrane pressure varied from 0.5 to 2 bars while the cross-flow velocity is varied from 1.2 to 4 m/s (Carrere et al., 1998). The amount of glucose that has been filtered can be determined by using Dinitrosalicylic Colorimetric Method (DNS). The optimization of glucose separation can be done by the Response Surface Methodology (RSM). This method decrease the period of research instead of maximizes the response.

1.5   RATIONALE AND SIGNIFICANCE OF STUDY

Raw material used can be considered as a low cost because sawdust was abundant and inexpensive in Malaysia. The composition of the cellulose is plenty in sawdust. The reuse of sawdust can also reduce the environmental pollution. Besides that, the production of cellulose has a potential in a future because from the cellulose, many valuable product can be produce such as bio-ethanol. Membrane separation was chosen because it has been widely used and has successfully proven its efficiency in various type of industry. However, there was lacking of membrane reactor used for separation of glucose from cellulose hydrolysates. Membrane reactor is the best method to separate glucose from cellulose hydrolysate as the enzyme cellulase and cellobiase will be neglected back to the reactor.

CHAPTER 2

LITERATURE REVIEW

2.1   RAW MATERIAL

Cellulose, like starch, is a polymer of glucose. However, unlike starch, the specific structure of cellulose favors the ordering of the polymer chains into tightly packed, highly crystalline structures that is water insoluble and resistant to depolymerization. The other carbohydrate component in lignocellulosics is hemicellulose, which, dependent on the species, is a branched polymer of glucose or xylose, substituted with arabinose, xylose, galactose, fucose, mannose, glucose, or glucuronic acid (Mosier et al., 2005). Pretreatment is an important tool for practical cellulose conversion processes, and is the subject of this article. Pretreatment is required to alter the structure of cellulosic biomass to make cellulose more accessible to the enzymes that convert the carbohydrate polymers into fermentable sugars (Mosier et al., 2005).

Lignocellulose is the primary building block of plant cell walls. Plant biomass is mainly composed of cellulose, hemicellulose, and lignin, along with smaller amounts of pectin, protein, extractives (soluble nonstructural materials such as nonstructural sugars, nitrogenous material, chlorophyll, and waxes), and ash (Jorgensen et al., 2007). The composition of these constituents can vary from one plant species to another. For example, hardwood has greater amounts of cellulose, whereas wheat straw and leaves have more hemicellulose (Sun and Cheng, 2002). Lignin is a complex, large molecular structure containing cross-linked polymers of phenolic monomers. It is present in the primary cell wall, imparting structural support, impermeability, and resistance against

microbial attack (Perez et al., 2002). Figure 2.1 shows the role of pretreatment in conversion of biomass.
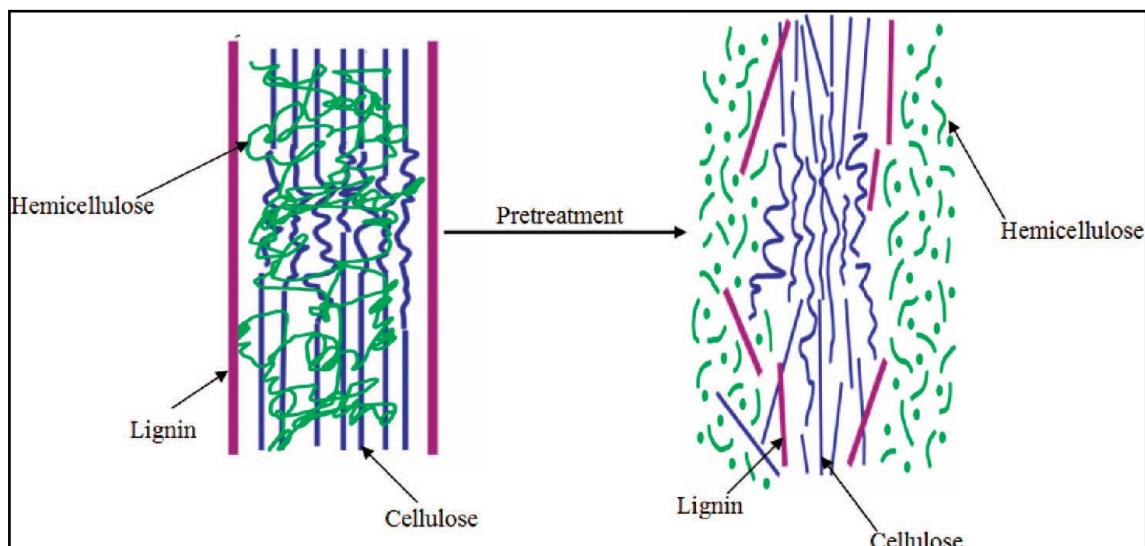
Figure 2.1: Schematic of the role of pretreatment in conversion of biomass

Source: Kumar et al., (2009)

In general, prospective lignocellulosic materials for fuel ethanol production can be divided into six main groups namely crop residues such as sugarcane bagasse, corn stover, wheat straw, rice straw, rice husks, barley straw, sweet sorghum bagasse, olive stones and pulp, hardwood such as aspen and poplar, softwood such as pine and spruce, cellulose wastes such as newsprint, waste office paper and recycled paper sludge, herbaceous biomass such as alfalfa hay, switch grass, reed canary grass, coastal Bermuda grass and timothy grass. Lignocellulosic biomass typically contains 55–75% carbohydrates by dry weight (Mosier et al., 2005). The carbohydrate content consists of mainly three different types of polymers, namely cellulose, hemicelluloses and lignin, which are associated which each other (Hendriks and Zeeman, 2009). Table 2.1 shows the general composition of selective lignocellulosic biomass containing cellulose, hemicelluloses and lignin.

Table 2.1: Cellulose, Hemicelluloses and Lignin contents in lignocellulosic biomass

Lignocellulosic material	Cellulose (%)	Hemicellulose (%)	Lignin (%)
Hardwood stems	40-55	24-40	18-25
Softwood stems	45-50	25-35	25-35
Nut shells	25-30	25-30	30-40
Corn cobs	45	35	15
Grasses	25-40	35-50	10-30
Paper	85-99	0	0-15
Wheat straw	30	50	15
Sorted refuse	60	20	20
Leaves	15-20	80-85	0
Cotton seed hairs	80-95	5-20	0
Newspaper	40-55	25-40	18-30
Waste papers from chemical pulps	60-70	10-20	5-10
Primary wastewater solids	8-15		2.7-5.7
Solid cattle manure	1.6-4.7	1.4-3.3	
Coastal Bermudagrass	25	35.7	6.4
Switch grass	45	31.4	12
Swine waste	6	28	N/A

Source: Kumar et al., (2009)

2.2 PRETREATMENT AND RECOVERY OF LIGNOCELLULOSIC BIOMASS

Lignocellulosic biomass is mainly composed of cellulose, hemicelluloses and lignin. Cellulose was hydrolyzed to its monomeric constituents during enzymatic hydrolysis and then fermented to ethanol or other products. The cellulose biodegradation by cellulolytic enzymes is slow because of the networks between lignin-hemicelluloses were embedded the cellulose fibers. Therefore, pretreatment process is important to remove lignin and hemicelluloses, reduce cellulose crystallinity, and

increase the porosity of the materials (Sun and Cheng, 2002) so that the produced cellulose is suitable for enzymatic hydrolysis. Pretreatment is required to disrupt the structure of lignocellulosic materials during cellulosic ethanol production, because the extensive interactions among cellulose, hemicelluloses and lignin, and the barrier nature of lignin minimize enzyme access to the carbohydrates and result in poor yields of fermentable sugars.

In general, pretreatment methods can be roughly divided into different categories such as physical pretreatment, physicochemical pretreatment, chemical pretreatment, biological, electrical, or a combination of these. The following pretreatment technologies have promise for cost-effective pretreatment of lignocellulosic biomass for biological conversion to fuels and chemicals (Kumar et al., 2009). Some pretreatment combines any two or all of these pretreatment and can be produce subcategories. Biological pretreatment has not attach much attention probably because of kinetic and economic considerations although there have been various research showing biological pretreatment can be an effective way to recover sugars from different species of biomass.

Physical and chemical pretreatments have been the subject of intensive research. Steam and water are usually excluded from being considered as chemical agent for pretreatment, since no extra chemical are added to the biomass. Physical pretreatment include comminuting, in which the particle sizes of the biomass are reduced with mechanical forces, steam explosion, and hydrothermalysis. Acids or bases promote hydrolysis and improve sugar recovery yield from cellulose by removing hemicelluloses and lignin during pretreatment. Sulfuric acid and sodium hydroxide are the most commonly used acid and base, respectively. Another approach for pretreatment is to use liquid formulations capable for acting as solvent for cellulose. Works with cellulose solvent systems have shown the enzymatic hydrolysis could be greatly improved, but the works mainly have been restricted to agricultural residues and herbaceous grass.

One of the main problems during the pretreatment and hydrolysis of biomass is the variability in the content of lignin and hemicelluloses. This variability depends on factors as the type of plant from which the biomasses obtained, crop age, method of

harvesting, etc. this makes that no one of the pretreatment methods could be applied in a generic way for many different feed stocks. The future trends for improving the pretreatment of lignocellulosic feed stocks also include the production of genetically modified plant materials with higher carbohydrate content or modified plant structure to facilitate pretreatment in milder conditions or using hemicellulases. Several studies have shown the potential of sodium hydroxide pretreatment on a variety of lignocellulosic materials.

Furthermore, sodium hydroxide can enhances lignocelluloses digestibility by increasing internal surface area, decreasing the degree of polymerization and the crystallinity of celluloses, and separating structural linkages between lignin and carbohydrates effectively. Besides that, the digestibility of sodium hydroxide treated hardwood increased with the decrease of lignin content (Wang et al., 2010). Otherwise, the porosity of the lignocellulosic materials increases with the removal of the cross links which is lignin (Sun and Cheng, 2002). The major effect of alkaline pretreatments is the delignification of lignocellulosic biomass, thus enhancing the reactivity of the remaining carbohydrates (Wang et al., 2010). Besides that, based on the prominently researched and promising technology, dilute acid pretreatment was chosen as the method for treatment. The function of acid in this pretreatment is to break down the hemicelluloses and opens the remaining structure for subsequent enzymatic hydrolysis. Furthermore, reaction conditions which favor the production of xylose monomer while minimizing degradation to furfural is preferred so as they do not inhibit subsequent enzymatic hydrolysis.

Pretreatment of biomass with dilute sulfuric acid at high temperatures can effectively dissolve the hemicelluloses and increase the enzymatic digestibility of celluloses. Besides that, the pretreatment can be performed at the moderate temperature. These two conditions give different xylose yield as well as the glucose yield. However, the dilute acid pretreatment still give significant results based on the production of xylose and glucose. The reaction time can be extended to obtained higher yield of sugar with a period from days to week. The advantages of the dilute sulfuric acid were high reaction rates, low acid consumption, and low cost of sulfuric acid. Dilute sulfuric acid pretreatment is deserving attention due to relatively inexpensive and to produce high

hemicelluloses recoveries and cellulose digestibilities (Lee et al., 2009). Therefore it has been assayed on a variety of substrates.

The application of dilute acid pretreatment to woody biomass can achieve some level of success so that can provide satisfactory cellulose conversion with certain hardwood species (Zhu and Pan, 2009). The dilute sulfuric acid pretreatment can effectively solubilized hemicelluloses into monomeric sugars, thus improving cellulose conversion. Compared to other pretreatment methods, it is especially useful for the conversion of xylan in hemicelluloses to xylose that can be further fermented to ethanol by many microorganisms (Sun and Cheng, 2005). Otherwise, dilute sulfuric acid pretreatment is effective because it is relatively inexpensive and due to high hemicelluloses recovery and cellulose digestibility (Cara et al., 2008). Besides that, dilute acid pretreatment with sulfuric acid has been extensively researched because it is inexpensive and effective, although other acid such as nitric acid, hydrochloric acid and phosphoric acid has also been tested (Hu et al., 2008).

2.3   GLUCOSE (PRODUCT)

Glucose is by far the most common carbohydrate and classified as a monosaccharide, an aldose, a hexose, and is a reducing sugar. It is also known as dextrose, because it is dextrorotatory; meaning that as an optical isomer is rotates plane polarized light to the right and also an origin for the D designation.

Glucose can be thought of as a derivative of hexane (a 6-carbon chain) with -OH groups attached to every carbon except the endmost one, which exists as an aldehyde carbonyl. However because the chain is flexible it can wrap around until the 2 ends react together to form a ring structure. Thus a solution of glucose can be thought of as a rapidly changing mixture of rings and chains, continually inter converting between the 2 forms.

In reality, an aqueous sugar solution contains only 0.02% of the glucose in the chain form, the majority of the structure is in the cyclic chair form. Since carbohydrates contain both alcohol and aldehyde or ketone functional groups, the straight-chain form is easily converted into the chain for, hemiacetal ring structure. Due to the tetrahedral

geometry of carbons that ultimately make a 6 member stable ring, the OH on carbon 5 is converted into the ether linkage to close the ring with carbon 1. This makes a 6 member ring which had five carbons and one oxygen.
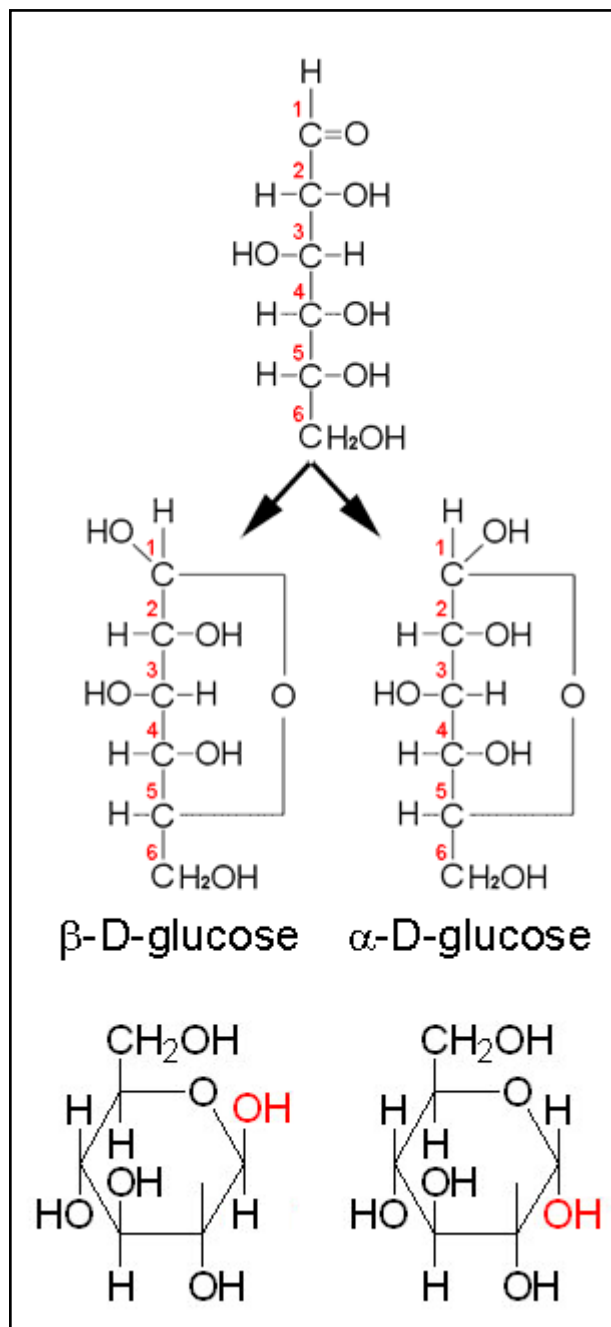
Figure 2.3: Structure of glucose

Source: http://alevelnotes.com/Monosaccharides/64

2.4   SEPARATION OF LIGNOCELLULOSIC BIOMASS RECOVERY

Separation processes such as sedimentation, filtration, membrane separation and centrifugal separations can be used for fractionating the wood extract. For the success of any molecular or ionic separation process downstream from wood hydrolysis and extraction, the extracts must be relatively clean and particles free (Duarte et al., 2010). This is particularly important since fouling and flux decay in nanofiltration or reverse osmosis applications can render these separations unviable on large scale.

Research has been conducted by Alriols et al., (2010) on the combined organosolv ethanol pretreatment with membrane ultrafiltration technology to treat the non-woody biomass feedstock of the species *miscanthus sinensis*. The lignin fraction with specific molecular weight was obtained by membrane ultrafiltration as it proportioned excellent fractionation capability with low chemicals consumption and low energy requirements. Besides that, acetic acid produced from the hydrolysis of herbaceous biomass such as corn stover was conventionally being separate and removed by chromatography method using resin column. Due to certain limitation, adsorptive microporous membrane has been used to remove acetic acid from corn stover hydrolysates (Wickramasinghe et al., 2008).

Furthermore, the separation of hemicelluloses from wood hydrolysates has been reported (Mohammad, 2008). The retention of hemicelluloses using two filtration steps was found to almost complete where the fouling ability of the used membrane was relatively low. The flux obtained at the first filtration was 165 kg/m^2.h at 1 bar with 18% of membrane fouling and 24 kg/m^2.h of flux at 10 bars with 30% of membrane fouling at second filtration.

2.5   MEMBRANE PROCESS

Membrane processes are mass transfer unit operations utilized for separation process either liquid-liquid or gas-liquid mixtures. Membrane is an ultra thin semi permeable barrier separating two fluids and allows the transport of certain species through the barrier from one fluid to the other. It is this permeability that gives the

membrane its utility and potential to separate a variety of process streams. The most universally employed membranes are composed of organic polymers. Otherwise, type of membrane from metal, ceramic, liquid and gas membranes are also used. In all membrane methods, the membrane separates the fluid passing through it into a permeate (that which passes through) and a retentate (that which is left behind). When the membrane is chosen so that it is more permeable to one constituent than the other, then permeate will be richer in the first constituent than the retentate (Kumar et al., 2010).

2.6   MEMBRANE SEPARATION OF GLUCOSE

Color removal from sugar syrup and the improvement of its sugar purity using ultrafiltration has great advantage. Membrane separation has been studied for color removal from green sugar syrup (Gyura et al., 2005). Ultrafiltration membranes with porosity ranging from 6 to 20 kilo Dalton (kDa) were used to remove color from raw 16 sugar cane solution. The permeate was decolorized by 58% using a 6 to 8 kDa membrane at a flux of 35.32 $L/m^2.h$, which gave the best results. The 15 to 20 kDa membrane only removed 50% of the color at a flux of 15.78 $L/m^2.h$.

Membrane separation has been performed as an alternative method for the recovery of xylitol from the fermentation broth of hemicelluloses hydrolysates because it has the potential for energy savings and higher purity (Affleck, 2000). A 10,000 nominal molecular weight cutoff (MWCO) polysulfone membrane was found to be the most effective for the separation and recovery of xylitol. The membrane allowed 82.2 to 90.3% of xylitol in the fermentation broth to pass through the membrane.

Otherwise, membrane filtration has also been used as an alternative for the separation and purification of hemicelluloses extracted from wood and annual crops (Mohammad, 2008). The outcome shows that the permeate flux through ultrafiltration and tight ultrafiltration membranes was relatively high. The fouling ability of the used membranes was relatively low. In addition, the retention of hemicelluloses using two filtration steps was almost complete.
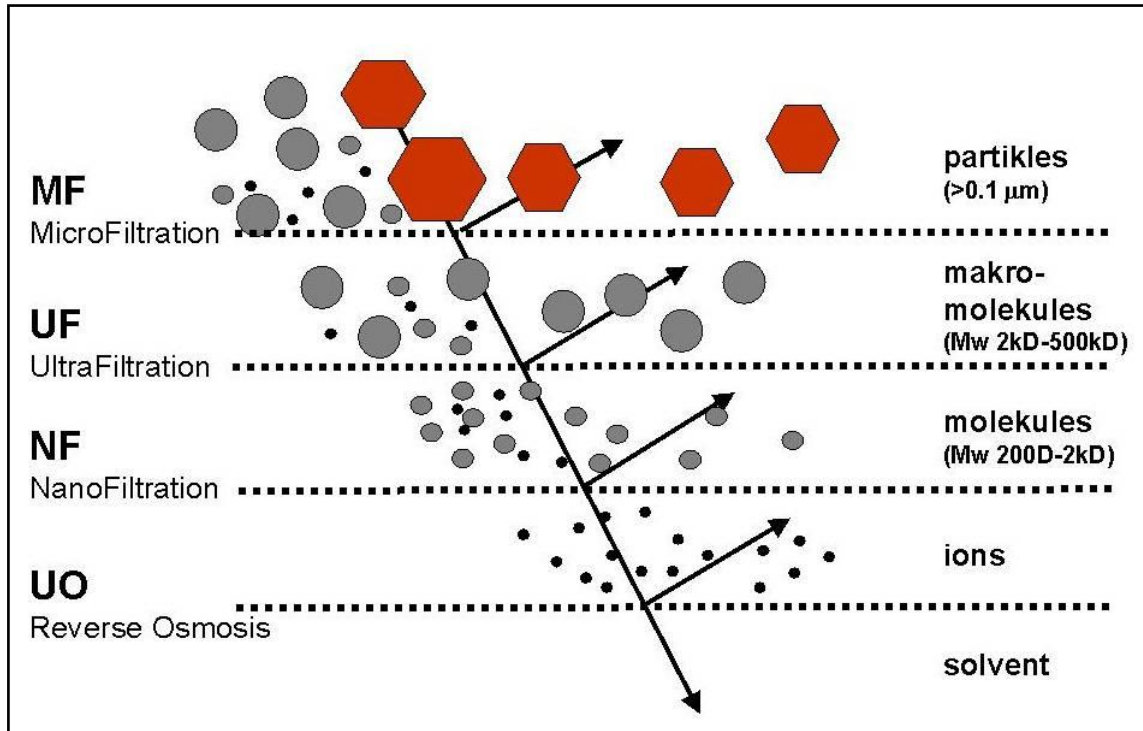
Figure 2.4: Separation characteristics for pressure driven membranes

Source: http://www.ps-prozesstechnik.com/en/membrane-technology.html

Membrane technology is used to recycle the valuable materials and purify the process water for reuse purposes in pulp and paper industry. Several related studies performed membrane filtration to isolate hemicelluloses from process water of thermo-mechanical pulping.

The membranes available were different in types and come in variety of characteristics which depend on membrane material and the process condition during manufacture. The nominal molecular weight cutoff and pore size defines some membranes performances. Membranes will reject certain molecules based on its categorized. Each membrane category can be used to filter solutions and perform different separation tasks. Membranes are generally classified into the categories ranging from microfiltration and ultrafiltration to nanofiltration and reverse osmosis.

The major differences between each of these categorized membranes are the nominal molecular weight cutoff (MWCO). The MWCO is based on the spherical shape of the protein molecules and can change with different shape molecules such as, polysaccharides (Affleck, 2000). Microfiltration membranes are classified with pore size ranging from 0.1 μm to 5 μm. Ultrafiltration membranes are classified with pore sizes up to 100 nm which used to reject molecules with molecular weight above 1000. Nanofiltration membranes have MWCO ranging from 300 to 1000, while reverse osmosis membranes are used for removing salts and larger impurities. Figure 2.4 shows the separation characteristics for pressure driven membranes.

2.6.1   Microfiltration

This membrane process closely resembles conventional filtration. Microfiltration (MF) can be used to separate suspended particles from solutions. The membranes are designed to reject particles in the micron range from 0.1 μm to 5 μm that means the suspensions and emulsions can be retained. The separation is usually based on solute particles dimensions specifically size and shape. MF can be used for removing particles from liquid or gas streams, purification of water, clarification and wastewater treatment (Affleck, 2000). Removal of suspended solids is the typical application of microfiltration. It can be used as cleaning step in clarification of fruit juice or cold sterilization of beverages and pharmaceutical and also as concentration step such as cell harvesting (Mohammad, 2008). Microfiltration is sometimes used as a pre-treatment step for nanofiltration and reverse osmosis for the production of potable water from ground or surface water, and ultra-pure water in the semiconductor industry.

Materials used to make microfiltration membranes include polypropylene, regenerated cellulose and polyvinyl chloride. Synthetic polymeric membranes can be divided into two classes which are hydrophobic and hydrophilic. The fouling tendency is higher in hydrophobic membrane, especially in proteins separation. Furthermore, water can not pass through some very hydrophobic membranes so they can not be wetted by water. In this case, alcohol can be good alternative to pretreat this membranes prior use them with aqueous solutions (Mohammad, 2008).

2.6.2 Ultrafiltration

Ultrafiltration can be broadly defined as a method for concentrating and fractionating macromolecules where a membrane acts as a selective barrier. Ultrafiltration employs membranes whose pore size typically ranges from 5 to 100 nm, with a MWCO above 1,000. Polysulfone and polyethersulfone are commonly used to make ultrafiltration membranes. Some factors that affect the separation in ultrafiltration membranes are the membrane type and characteristics, transmembrane pressure, pH of the feed, and the protein concentration in the feed (Affleck, 2000).

Materials and conditions used can control how large the pores of the membrane are and consequently what molecules and particles can pass through the membrane. The transmembrane pressure is the driving force for flux and is measured as the average of the inlet and outlet pressure, minus the pressure on the permeate side of the membrane. Permeate rates are measured in flux, which is the amount of fluid passing through the membrane and is usually given in terms of volume per unit time per unit membrane area (Affleck, 2000). From Equation 1, the parameters applied to identify the flux declination and the efficiency of membrane processes are as follows:

$$J = \frac{Q}{A} \tag{2.1}$$

where *J* is the flux through the membrane (LMH), *Q* is the permeate flow rate (LPM) and *A* is the effective membrane area (m2) (Sakinah *et al.*, 2007).

The membrane separation of cheese whey was evaluated by using two criteria which are permeate flux and protein retention. From equation 2.2, the permeate flux was calculated by measuring the quantity of permeate collected during a certain time and dividing it by the effective membrane area for filtration (Li et al., 2006).

Permeate flux,

$$J = \frac{\text{permeate volume}}{\text{membrane area x time}} \; (Lm^{-2}h^{-1}) \tag{2.2}$$

Cross flow ultrafiltration has been used to separate microbial cells and protein from fermentation broths (Li et al., 2006). At the initial stage of cross flow filtration the yeast cells and other particles were deposited on the membrane to form a cake similar to dead-end filtration. The flux through the ultrafiltration membrane rapidly decreased in the first 15 minutes of filtration and then steady state was achieved after the initial microbial cake was deposited on the membrane.

2.6.3 Nanofiltration

Nanofiltration (NF) refers to a filtration process with a membrane MWCO of 300 to 1,000. For such membranes, the MWCO falls in the separation domain situated between reverse osmosis and ultrafiltration. Unlike reverse osmosis, the retention of salts in nanofiltration is low for molecular weight below 100; it is high for organic molecules of molecular weight above 300 (Affleck, 2000).

Nanofiltration membranes have been commercially manufactured. Nanofiltration membranes are capable of concentrating sugars, divalent salts, bacteria, proteins, particles, dyes, and other particles with molecular weight greater than 1000. Nanofiltration membranes reject molecules based on size when the particles are too large to pass through the pores. In addition, nanofiltration membranes can also use charge to reject molecules, much like reverse osmosis (Affleck, 2000).

The most promising application for nanofiltration is purification of ground water and surface water. This process is applied to retain micro-pollutants such as herbicides, and insecticides. Generally, the retention of low molar mass organics in the range of 200 to 1000 g/mol, and multivalent salts such as calcium salts can be achieved by NF. The driving pressure that usually applied in NF processes is in the range 3- 20 bars. The industrial applications of NF are the concentration of product streams with specific components such as proteins, enzymes, antibiotics and dyes. NF is also used to separate low molar mass solutes such as inorganic salts or small organic molecules such as glucose, and sucrose from a solvent. NF membranes can be used for softening the hard water (Mohammad, 2008).

2.6.4   Reverse Osmosis

Reverse osmosis (RO) is the process of forcing water through a membrane from a more concentrated to less concentrated aqueous solution. Reverse osmosis utilizes extremely fine pores in the membranes that are typically made from cellulose acetate. The pores are believed to be less than 0.001 μm in diameter. However, reverse osmosis is not filtration. Filtration is the removal of particles by size exclusion or the particles are too large to go through physical pores. In the case of reverse osmosis, such pores have never been viewed with a microscope. It is more likely that the small molecules permeate the reverse osmosis membrane by diffusive forces (Affleck, 2000).

The retention of all low molar mass solutes can be achieved by RO. The RO membranes are used in desalination of seawater. High potable water recovery can be obtained from seawater in single stage operation. Since the osmotic pressure increases in the retentate side, high applied pressure ranging from 20-100 bars is required. The average hydrodynamic pressure in the seawater desalination process is about 60 bars. This pressure can be enough to exceed the osmotic pressure of seawater that is around 25 bars (Mohammad, 2008).

Retention of low molar mass solvents such as methanol and ethanol is fairly good by RO. However, the rejection of the solutes by RO strongly depends on the type of the membrane. The main industrial applications of the RO are production of ultra-pure water for electronic industry, concentration of fruit juice and sugars in food industry, and concentration of milk in dairy industry (Mohammad, 2008).

Both asymmetric and composite membranes are used for RO. The structure of the latter membranes is denser than NF membranes. The top layer is formed by interfacial polymerization reaction. Polysulfone or polyethersulfone, cellulose triacetate and aromatic polyamides are usually used to form support layer of the RO membrane (Mohammad, 2008).

2.7   MEMBRANE FOULING

It is clearly expected that as cross-flow velocity increases, the mass and thickness of each fouling layer should decrease, resulting in decreased filtration resistance (Hyeok et al., 2005). Membrane fouling in a cross-flow ultrafiltration unit can be minimised by increasing the cross-flowvelocity or decreasing the operational transmembrane pressure. However, both of these techniques decrease the net productivity of the system (Paul et al., 2006). Along with the increased membrane surface cross-flow velocity, the trans- membrane pressure also increased. When the membrane surface velocity reached 1.6 m/s, the foulant on the surface was peeled off by the flow perpendicular to permeate directly; meanwhile, it was difficult for the foulant to settle perpendicularly due to the high velocity flow. Therefore, the transmembrane pressure could be controlled, but it had the disadvantage of a greater return flow (Lei et al., 2008). During the process of membrane filtration, the fouling layer is formed. So with the progress of membrane filtration, the transmembrane pressure gradually increases, in the meantime, the permeated water quality of the membrane remains steady on the whole which indicates that the fouling layer plays a filtration function as the membrane itself (Lei et al., 2008).

Many studies have been carried out to understand and control membrane fouling. Puro et al., (2010) has stated that the easiest way to optimize the filtration process to ensure a low-fouling process is to choose an optimal membrane for filtration. Otherwise, the major membrane characteristics that affect fouling are charge, morphology and hydrophilicity. To solve this problem, a great deal of anti-fouling studies, such as blending, coating, adsorption, chemical-grafting, and radiation induced grafting, have been invented to modify the membrane (Liang et al., 2010). However, there are also studies on the operating and process conditions to control the membrane fouling such as solution pH, solution concentration, ionic strength, stirring speed, transmembrane pressure, cross flow velocity, temperature, etc. Among all the operating parameters, the transmembrane pressure and cross flow velocity are the most important parameters that influence to control the membrane fouling.

2.7.1   EFFECT OF TRANSMEMBRANE PRESSURE (TMP)

Transmembrane pressure has also been studied as operating parameter to measure and control the membrane fouling. Research on the separation of proteins from an aqueous solution by dead end filtration has been conducted to determine the effect of solution pH, initial protein concentration, transmembrane pressure, ionic strength and stirring speed (Lin et al., 2008).

Effective separation was achieved at a lower protein concentration, a lower TMP or a lower pH. Thomassen et al., (2005) has studied the fouling propensity during cross flow filtration of a model beer, primarily composed of dextrin and protein. An increase in transmembrane pressure resulted in a reduction in transmission of both the BSA protein and dextrin components of the model beer for a given cross flow velocity while an increase in cross flow velocity led to increased transmission of both the BSA and dextrin through the membrane for a given transmembrane pressure. Otherwise, the permeate flux of both ceramic and polyvinylidene difluoride (PVDF) ultrafiltration membranes decreased with filtration time until it reached steady-state values (Ahmad et al., 2005).

2.7.2   EFFECT OF CROSS FLOW VELOCITY (CFV)

Studies have been conducted by several researches to reduce the fouling on membrane during the separation process. Cross flow velocity is used to reduce the effect of additional resistance due to concentration polarization and fouling or gel layer on the membrane surface (Mohammad, 2008). The influence of the concentration polarization and fouling in microfiltration might cause a dramatic permeate flux decline comparing with pure water flux.

Hwang and Sz, (2010) has been studied on the operating condition on the filtration flux for solute rejection and membrane fouling in BSA/dextran binary suspension cross-flow microfiltration. The filtration flux was increased 30–50% by increasing the cross-flow velocity or transmembrane pressure. Besides that, cross flow velocity also influence on the formation of fouling layer during microfiltration and ultrafiltration during biological suspension (Choi et al., 2005). The formation of a reversible fouling layer was actually

prevented by a cross-flow velocity of 3.0 m/s for microfiltration membrane and 2.0 m/s for ultrafiltration membrane.

Fouling and regeneration of ceramic membranes used in recovering titanium silicalite-1 catalysts has been studied (Zhong et al., 2007). Estimation of hydrodynamic forces acting on a single particle shows cross flow velocity (CFV) has an important effect on the deposition of TS-1 particles. However, after particles have deposited, increasing CFV will not resuspend them due to the strong and dense cake layer formation.

2.8   MEMBRANE CLEANING

Membrane cleaning is performed due to the occurrence of fouling either reversible or irreversible. Reversible membrane fouling can be removed by physical cleaning such as hydraulic backwashing. Another one is an irreversible membrane fouling which cannot be removed by physical cleaning but can be removed by chemical cleaning (Hashino et al., 2010).

Cleaning is usually performed in four forms either by physical, chemical, biological or enzymatic. Chemical cleaning means removing impurities by means of 26 chemical agents. Some of these cleaning agents are acid, alkali, surfactants, disinfectants and combined cleaning materials. Most of the cleaning method is performed by using the chemical cleaning. Backwashing is applied mostly to neutralize back the membrane.

Alkali-acid cleaning has been performed in cleaning the membrane during the filtration of cheese whey media (Li et al., 2006). Besides, the membrane used was cleaned in ultrasonic cleaner with 0.1 M NaOH for approximately 30 min in the separation of protein by dead-end filtration (Lin et al., 2008). The membrane was further cleaned by stored in the 0.05% sodium azide solution at 4ºC. Madaeni and Samieirad, (2010) were studied the use of acid, alkaline solution, surfactant and chelating agent on cleaning the membrane fouled in treatment of wastewater by reverse osmosis. They found that the acids were not effective in recovering the flux however,

the two stages of caustic and detergent. Cleaning agents such as NaOH-SDS followed by acidic agent such as HCl provided high effective membrane regeneration.

There is also a study on membrane cleaning using electric pulse with an automated rig on the membrane surface (Ahmad et al., 2002). The automated rig developed was proven to reduce the membrane fouling using electric pulse for both dead-end microfiltration and ultrafiltration processes. As the pulse duration and applied voltage increased, the average flux was also increased. Furthermore, two types of chemical cleaning which are 0.1 M NaOH and 0.1 M HCl were applied as to determine the solutions effectiveness during the cyclodextrin separation (Sakinah et al., 2007). The alkaline solution cleaning shows a higher removal of weak adsorption, which was about 11% more compared to the acidic solution cleaning. The dominant foulant was an organic element, which can be significantly removed effectively by alkaline cleaning rather than acidic cleaning.

2.9   RESPONSE SURFACE METHODOLOGY (RSM)

Response Surface Methodology (RSM) is used in optimizing the conditions of tested variables in maximizing the response of an experiment. Many reports revealed by using RSM, the response is maximized. Beside, the period of research also decreased. In other ways, RSM helps in saving time and money. In the factorial design of experiments, when responses and input variable factors (e.g., the cross flow velocity and transmembrane pressure) are continuous, it is very useful to consider the factor response relationship in terms of a mathematical model such as the response function.

For qualitative factors where there is no continuous link between the response and the levels of a factor, it is necessary to consider a comparison of the response between two levels of a qualitative factor. The factorial approach results in a considerable saving of time and materials devoted to the experiments (Lin et al., 2008). First, the factor that is independent of all simple effects of a factor is equal to its main effect. The consequences of variations in the factors and the main effects are the only quantities that need to be stated. Second, each main effect in factorial experiments is

estimated with the same accuracy as if the whole experiment had been devoted to the factor alone.

Thus, the advantages of this methodology contain (i) all experimental units are used in evaluating effects, resulting in the most efficient use of resources, (ii) the effects are evaluated over a wider range of conditions with the minimum of resources, and (iii) a factorial set of treatments is optimized for estimating main effects and interactions (Lin et al., 2008).

In general, the linear terms are more significant than the quadratic interactions. Results show that TMP and initial protein concentration are the most significant factors, and stirring speed is the less significant one in the present filtration process. It is noticed that the model parameters are determined by an ANOVA fitting exercise, so that the model could adequately describe most of the data (Lin et al., 2008).

CHAPTER 3

METHODOLOGY

3.1 GENERAL METHODOLOGY

Process flow for production and separation of glucose from cellulose hydrolysate was shown in Figure 3.1.
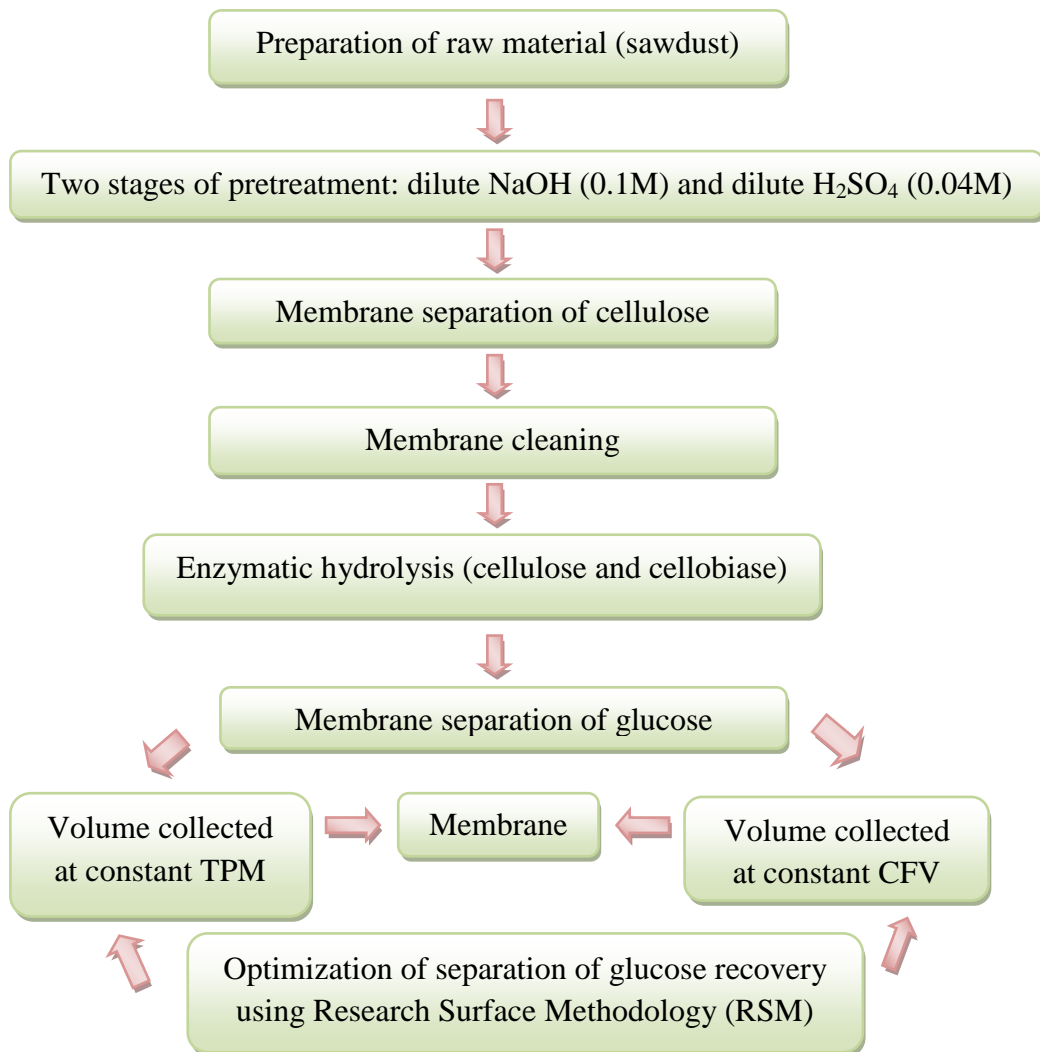
Figure 3.1: Process flow for glucose separation

3.2   CELLULOSE RECOVERY

3.2.1   Preparation of Raw Material

Raw material used was hardwood sawdust (Keruing). Hardwood sawdust was taken from the saw mill factory at Gambang, Pahang. For the preparation of sawdust before pretreatment, 10 kg of sawdust was grind using the blender to reduce the particle size and surface area. Sawdust was then sieved using shack sieve with a pore size of 2 mm to provide fine size class of sawdust as shown in Figures 3.2 and 3.3. After that sawdust was dried (Figure 3.4) in the oven at 60ºC about 24 hours. Then it was stored in seal bags (Figure 3.5) at room temperature until further process (Guo et al., 2007).

Figure 3.2: Sieving process

Figure 3.3: Sawdust before and after sieving

Figure 3.4: Drying the sawdust

Figure 3.5: Sawdust after autoclave process

3.2.2 Pretreatment Process

Two-stage of pretreatment was performed inside the membrane reactor. For sodium hydroxide (NaOH) pretreatment, 5 kg of sawdust was first weigh using electronic balance. The sawdust was then introduced into the membrane reactor. The prepared 0.1 NaOH solution was added into the membrane reactor. The solution mixture was allowed to mix to react and was stirred at impeller speed of 15-20 rpm. The pretreatment was then performed at 75 ºC for 24 hours respectively. For sulfuric acid (H_2SO_4) pretreatment, the remaining sawdust residue approximately 5 kg from NaOH pretreatment was first introduced into the membrane reactor (Figure 3.6). For sulfuric acid (H_2SO_4) pretreatment, the remaining sawdust residue (Figure 3.7) from NaOH pretreatment was first introduced into the membrane reactor. The prepared 0.04M (H_2SO_4) solution was filled into the membrane reactor. The solution mixture was allowed to mix to react and was stirred at impeller speed of 15-20 rpm. The pretreatment was then performed inside the membrane reactor at 75ºC for 24 hours respectively (Figure 3.9). Finished with the pretreatment, the sample was cooled at certain temperature before undergo membrane filtration process (Wang et al., 2008).

Figure 3.6: Sodium Hydroxide pretreatment in membrane reactor

Figure 3.7: Sawdust after Sodium Hydroxide pretreatment
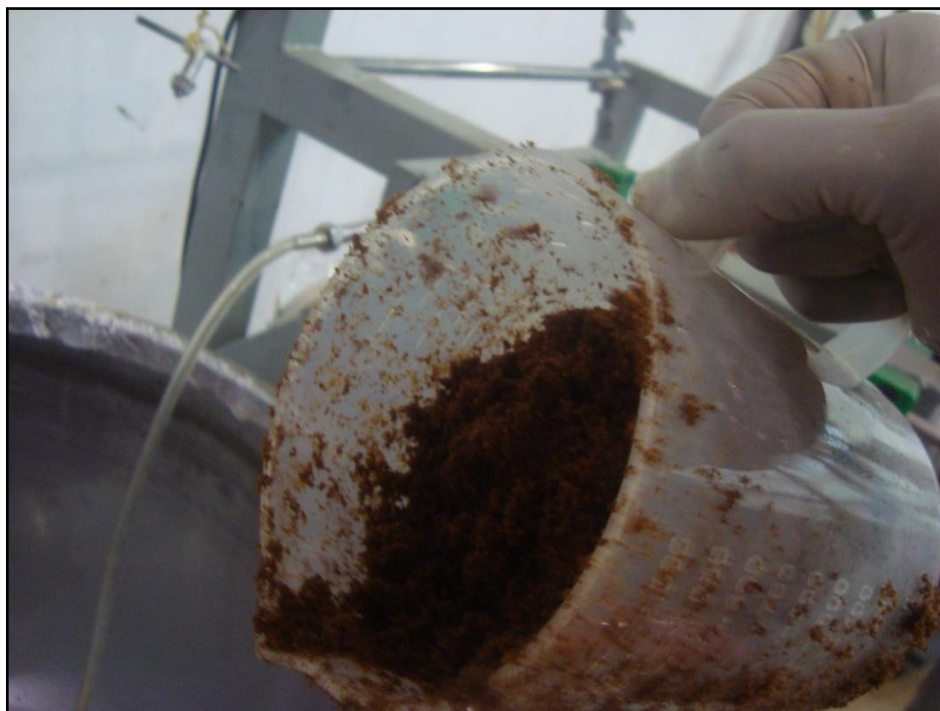
Figure 3.8: Pretreated sawdust (NaOH pretreatment) being introduced into membrane reactor

Figure 3.9: Sulfuric acid (H_2SO_4) pretreatment in membrane reactor

3.2.3 Membrane Separation of Cellulose

Membrane reactor system consists of membrane module, peristaltic pump, flow meter and pressure gauge was used for membrane filtration process. Submerged filter membrane was used during the experiment. The material of the membrane used was ceramic membrane with pore size of 0.9 μm and effective membrane area of approximately 0.03 m^2. The submerged membrane was horizontally assembled inside the membrane reactor. The membrane reactor consists of a stainless steel vessel with a mechanical stirrer attached (Sakinah et al., 2007). The mixing intensity of the process is 15-20 rpm. The membrane filtration of the solution mixture from dilute H_2SO_4 was performed. The process condition was at 50ºC with impeller speed of 15-20 rpm to enhance the separation process and to avoid fast membrane fouled. The membrane filtration was performed at optimum transmembrane pressure (TMP) at 1.0 bar and cross flow velocity 0.14 m/s respectively. The experiments were conducted at a constant temperature of 50°C.

3.2.4 Membrane Cleaning

The cleaning process involved backwashing with water and chemical cleaning with 0.05M NaOH solution. The first approached used where the membrane was flushed with water for about 5 to 10 minutes. Another approached by chemical cleaning was by soaked the membrane in 0.05M NaOH solution for overnight. The membrane was rinsed with water for several times before continue with the next experiment. Membrane appearance before and after filtration membrane cleaning were shown in Figure 3.10.
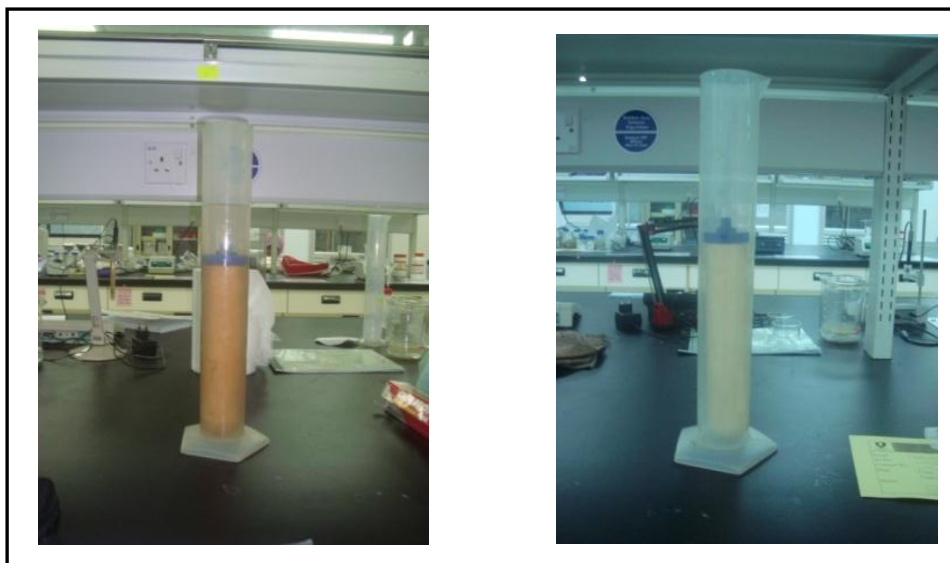
Figure 3.10: Membrane appearance before and after filtration membrane cleaning

3.3   GLUCOSE PRODUCTION

3.3.1   Enzymatic Hydrolysis

The enzymatic hydrolysis was carried out in the presence of 0.1 M sodium acetate buffer at pH 4.5. Sodium acetate buffer was prepared by mixing 13.95 liter of 0.2 M glacial acetic acid solution with 11.05 liter of 0.2 M sodium acetate solution and diluted with 50 liter of distilled water. Enzymes Cellulase and Cellobiase were loaded in the amounts of 50 μL /100 ml substrate respectively. The enzymatic activities condition was at 50ºC with impeller speed of 150 rpm to enhance the enzymatic activities. Enzymatic mixture was then performed inside the membrane reactor for 48 hours (Figure 3.11). Finally, the reaction mixture was filtered to separate the leftover biomass from the liquid fraction by using ultrafiltration membrane.
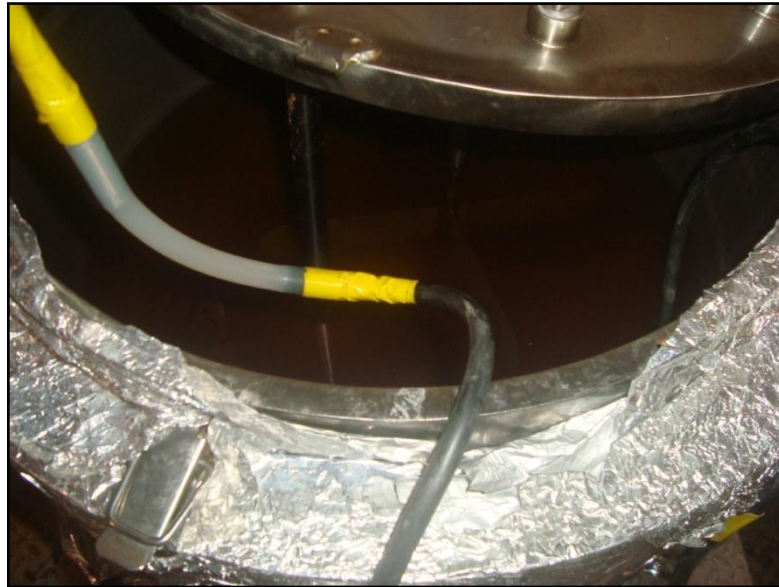
Figure 3.11: Enzymatic hydrolysis with cellulose and cellobiase

3.3.2 Membrane Separation of Glucose

The membrane filtration of the solution mixture from sodium acetate buffer was performed. The process condition was at 50ºC with impeller speed of 15-20 rpm to enhance the separation process and to avoid fast membrane fouled. As soon as the transmembrane pressure was decreased, the flux decreased and then increased in order to restore the previous steady state flux. The time needed to reach steady state varied from 25 to 40 min. The transmembrane pressure varied from 1.0 bar to 3 bars while cross flow velocity varied from 0.06 m/s to 0.22 m/s. The transmembrane pressure thus has an influence on the steady state flux, but it is very small (Carrere et al., 1998). The cross-flow velocity was varied from 1.2 to 4 m/s which led to a steady state flux polarisavariation from 4 to 7.3 $l\ h^{-1}\ m^{-2}$. The effect of cross-flow velocity was quite high. The time needed to reach steady state obtained within 30 min (Carrere et al., 1998). Separation of glucose using utrafiltration membrane was shown in Figure 3.12.

Figure 3.12: Separation of glucose using utrafiltration membrane

3.4 DINITROSALICYLIC COLORIMETRIC METHOD (DNS)

This method tests for the presence of free carbonyl group (C=O), the so-called reducing sugars. This involves the oxidation of the aldehyde functional group present in, for example, glucose and the ketone functional group in fructose. Simultaneously, 3,5-dinitrosalicylic acid (DNS) is reduced to 3-amino,5-nitrosalicylic acid under alkaline oxidations:

$$\text{Aldehyde group} \xrightarrow{\text{oxidation}} \text{carboxyl group} \tag{3.1}$$

$$\text{3,5-dinitrosalicyclic acid} \xrightarrow{\text{reduction}} \text{3-}\alpha \text{ min o,5-nitrosalicyclic acid} \tag{3.2}$$
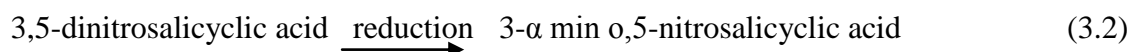
Due to the dissolved oxygen can interfere with glucose oxidation, sulfite, which itself is not necessary for the color reaction, is added in the reagent to absorb the dissolved oxygen (Wang, 2005).The details on how to prepare DNS solution (1%) was shown in Figure 3.13 and The details of the method were shown in Figure 3.14.

```
Equipment;
Test
Pipettes tubes
Spectrophotometer (UV VIS) + Cuvette
```

↓

```
Reagents;
DNS reagent solution (1%):
Dinitrosalisylic acid: 10.0gm
Phenol: 2.0gm
Sodium sulfite: 0.5gm
Sodium hydroxide: 10.0gm
De-ionized water: 1.0 Liter
Potassium sodium tartrate solution, 40%
```
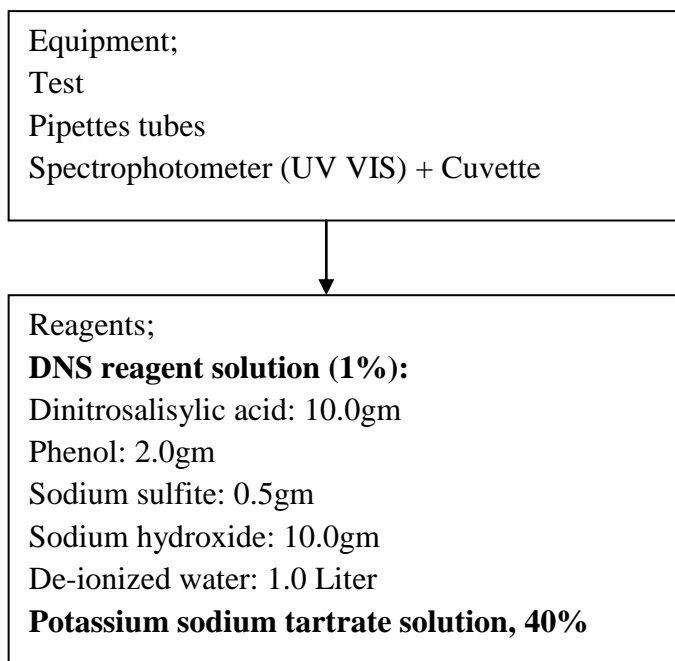
Figure 3.13: Preparation of DNS solution (1%)

```
3.0mL of DNS reagent was added to 3.0 mL of glucose sample
in lightly capped test tube (to avoid the loss of liquid due to
evaporation, cover the test tube with a piece of paraffin film if a
plain test tube is used)
```

↓

```
The mixture was heated at 90⁰C for 5 to 15 minutes to develop
the red brown color.
```

↓

```
1.0 mL of 40% potassium sodium tartrate (Rochelle salt)
solution was added to stabilize the color
```

↓

```
After cooling to room temperature in a cold water bath, the
absorbance was recorded with a spectrophotometer at 575 nm.
```

Figure 3.14: The procedures of the DNS method

Figure 3.15: UV Vis Spectroscopy

3.5   FOURIER TRANSFORM INFRARED SPECTROSCOPY (FTIR)

Mechanism reaction and esterification morphology of meranti sawdust, cellulose fibers, glucose and sugar alcohol were analyzed by means of Fourier Transform Infrared Spectroscopy (FTIR), (MODEL: THERMO) using a standard KBr pellet technique (Figure 3.16). The solid from sample was cut or homogenized particle from sample were weighing about 0.2 gm. The standard of KBr and sample were putted in the container and placed it into the FTIR test area. The KBr being analyzed using FTIR software as a background and then followed by materials as samples. Each spectrum was recorded with 64 scans in frequency range from $4000cm^{-1}$ to $400cm^{-1}$ with resolution $4cm^{-1}$.

Figure 3.16: Fourier Transform Infrared Spectroscopy

3.6 OPTIMIZATION OF GLUCOSE SEPARATION USING RESPONSE SURFACE METHODOLOGY (RSM)

The optimization can be done by the Response Surface Methodology (RSM). The low and high values from each parameter will be selected from the screening process. This method decrease the period of research instead of maximizes the response. Three-dimensional response surface and contour plots were generated to investigate the interactive effects of any two variables on the response by evaluating two variables at a time while holding the other one constant at central level. A three dimensional plot can give a clearer geometrical representation of the nature and extent of the interaction between the variables and response within the experimental range studied (Hui et al., 2010).

CHAPTER 4

RESULTS AND DISCUSSION

4.1   INTRODUCTION

In this chapter, the results obtained from the experiment were discussed. The experiment was performed to study the effect of transmembrane pressure (TMP) and cross flow velocity (CFV) on the permeate flux during the separation of cellulose recovery from sawdust wood hydrolysates. Besides that, the optimum TMP and CFV during membrane filtration was also studied. In order to achieve the objectives, the experiment was continued to the optimization of the separation of cellulose recovery using Response Surface Methodology (RSM).

4.2   EFFECT OF TRANSMEMBRANE PRESSURE (TMP) ON FLUX

In order to study the permeate flux decline, the experiment was performed at various transmembrane pressures (TMP) which values are at 1.0, 1.5, 2.0, 2.5 and 3.0 bars. The other variable which is cross flow velocity (CFV) was kept constant at 0.10 m/s in order to get the actual nature of dependence. The separation process was performed at 60 minutes duration at a temperature of 50 °C.

Figure 4.1: Flux pattern at TMP of 1.0 bar

Figure 4.1 shows the change in permeate flux over time under TMP of 1.0 bar. The plotted pattern shows that the permeate flux was decreased slowly for the first 15 minutes and later on decreased gradually before achieved the steady state flux at the last 15 minutes. The permeate flux was decreased for about 5.89% from 64.0806 L/m^2.h to 60.3023 L/m^2.h when the retention time is increased. The flux was decrease due to accumulation of flocculent on the surface of membrane. However, flux slightly increased at 45 minutes from 60.4156 L/m^2.h to 60.5206 L/m^2.h due to the unstable flow rate of the permeate that flow through the flow meter and also the pressure gauge reading that are not constant at 1.0 bar.
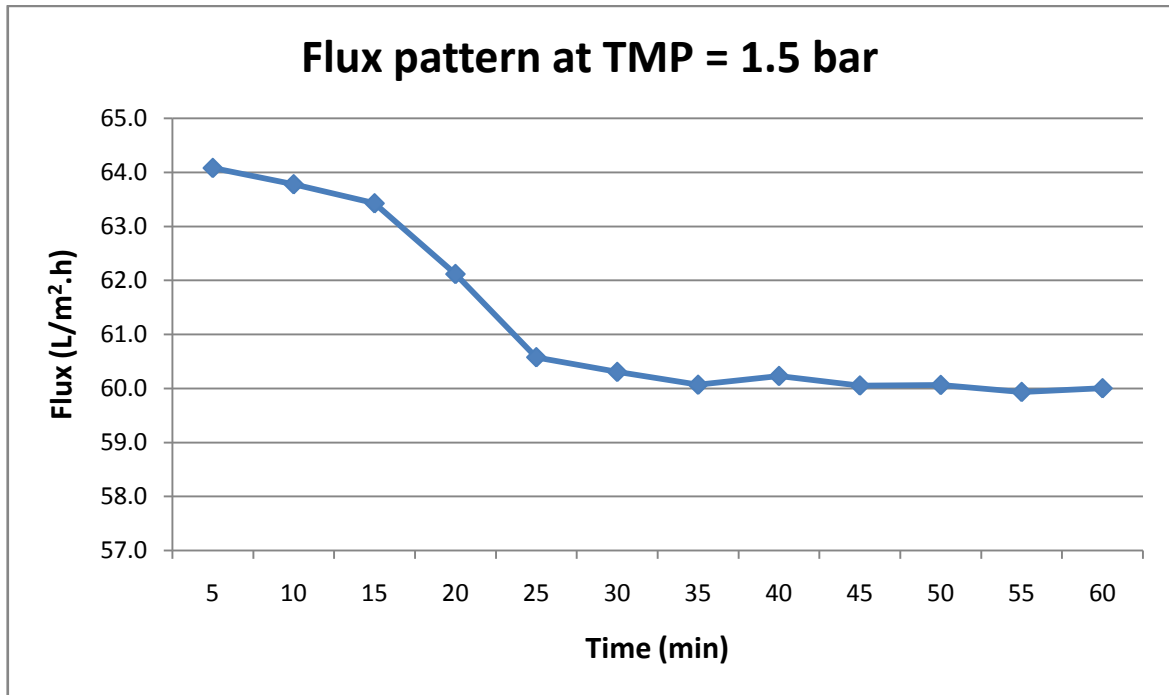
Figure 4.2: Flux pattern at TMP of 1.5 bar

Behavior on the permeate flux at TMP of 1.5 bar is shown in Figure 4.2. The plotted pattern shows that the flux was decreased slowly at the first 15 minutes. Later on, the flux was decreased gradually until it reaches the steady state condition at last 10 minutes. This shows that the flux was decreased to 6.37% from 64.0806 L/m^2.h to 60.0 L/m^2.h when the operating time is increased. Compared to flux pattern at TMP of 1.0 bar from Figure 4.1, percentage of flux decreased at TMP of 1.5 bar was slightly higher when increased the value of TMP. The decrease of the flux over time is a result of fouling of the membranes (Li et al., 2006). Fouling state at TMP of 1.5 bar started at first 35 minutes, compared to TMP of 1.0 bar from Figure 4.1 which started at first 40 minutes. It happened due to the increment in pressure that accelerates foulant accumulation process at membrane surface.
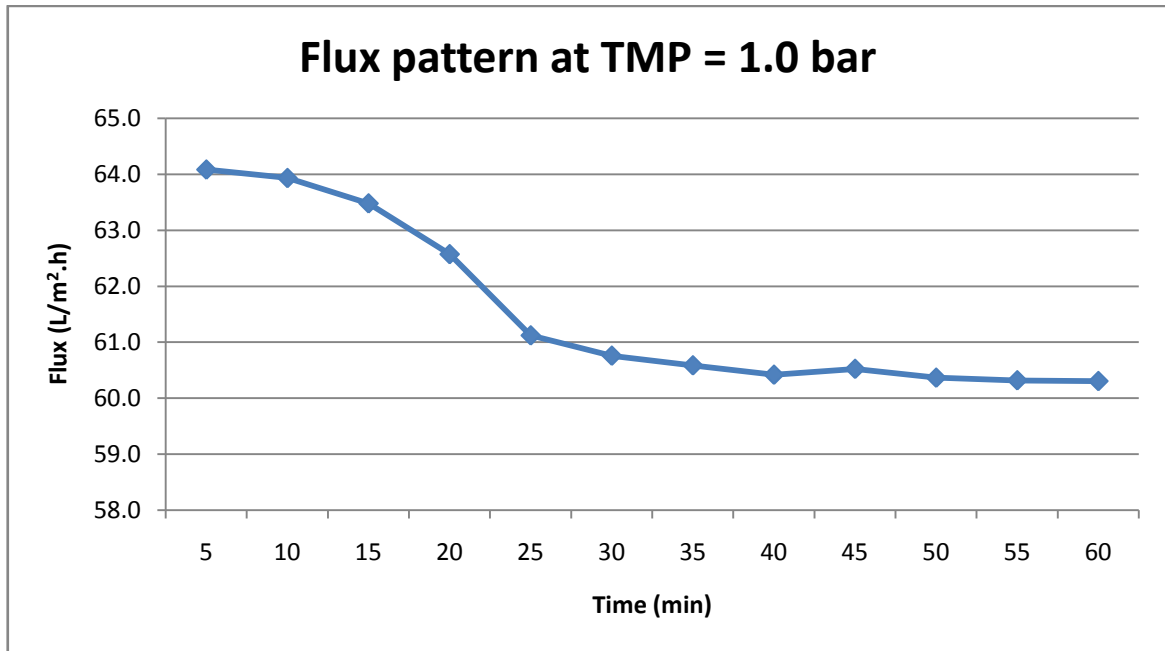
Figure 4.3: Flux pattern at TMP of 2.0 bar

Figure 4.3 shows the change in permeate flux over time at TMP of 2.0 bars. The plotted pattern shows that the permeate flux was constantly steady at the first 10 minutes, decreased at the next 5 minutes before continued decreased until it reaches the steady state at last 15 minutes. The flux was decreased to 7.23% from 63.7783 L/m^2.h to 59.1688 L/m^2.h when the operating time increased. The flux behavior was not consistent. This is because the operating condition is not stable and fluctuate during the experiment such as the permeate flow rate and the applied pressure which were not constant. Compared to flux pattern at TMP of 1.5 bar from Figure 4.2, percentage of flux decreased at TMP of 2.0 bar was slightly higher when increased the value of TMP. Fouling state at TMP of 2.0 bar started at first 30 minutes, compared to TMP of 1.5 bar from Figure 4.2 which started at first 35 minutes. It happened due to the increment in pressure that accelerates foulant accumulation process at membrane surface.
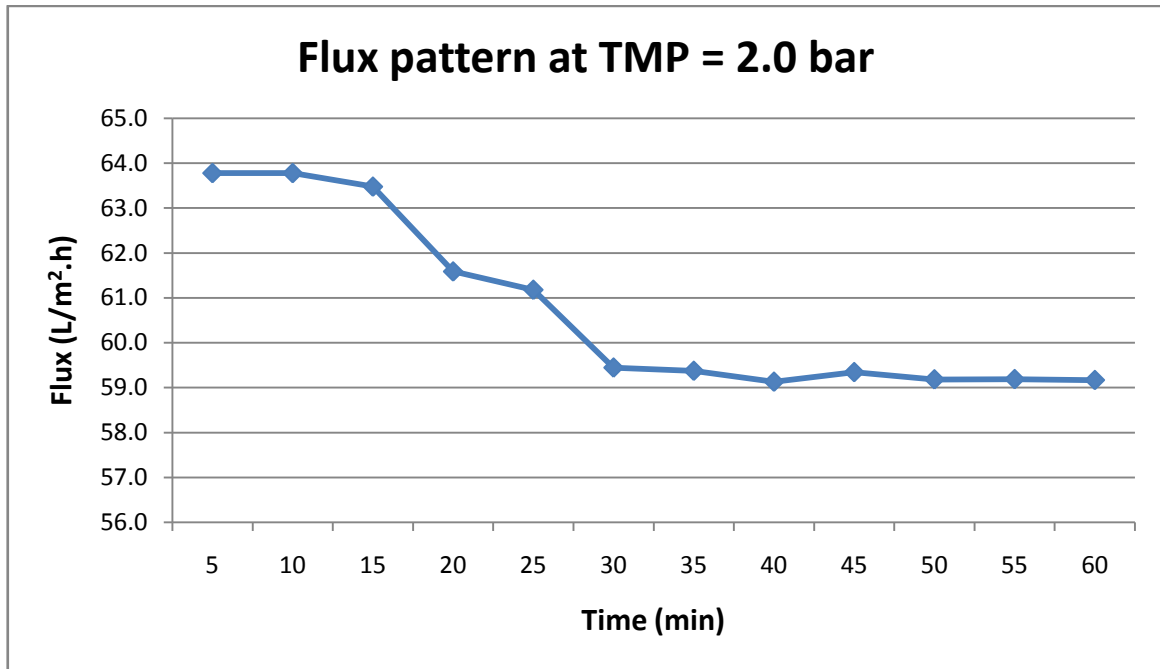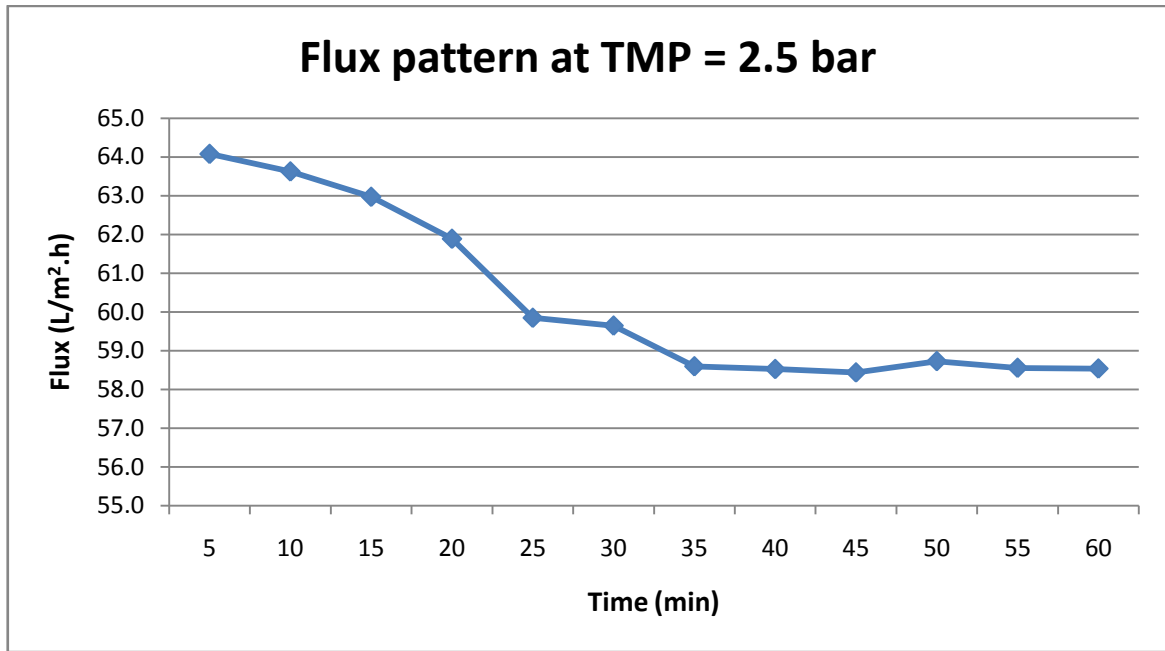
Figure 4.4: Flux pattern at TMP of 2.5 bar

From Figure 4.4, the flux pattern was obtained at the TMP of 2.5 bars. The pattern shows that the flux was decreased almost linearly over time. The decrement of flux is linear until it reaches the steady state at the last 20 minutes. The flux was decreased to 8.65% from 60.0806 $L/m^2.h$ to 58.5390 $L/m^2.h$ when the operating time increased. This was due to the fluctuated flow rate of the feed and unstable pressure gauge reading. Fouling state at TMP of 2.5 bar started at first 35 minutes, compared to TMP of 2.0 bar from Figure 4.3 which started at first 30 minutes. Theoretically, an increment in pressure will accelerates foulant accumulation process at membrane surface. However, due to the fluctuated flow rate of the feed and unstable pressure gauge reading to steadily maintain at TMP 2.5 bar causing late fouling state compared to TMP at 2.0 bar. Compared to flux pattern at TMP of 2.0 bar from Figure 4.3, percentage of flux decreased at TMP of 2.5 bar was slightly higher when increased the value of TMP. The decrease of the flux over time is a result of fouling of the membranes.
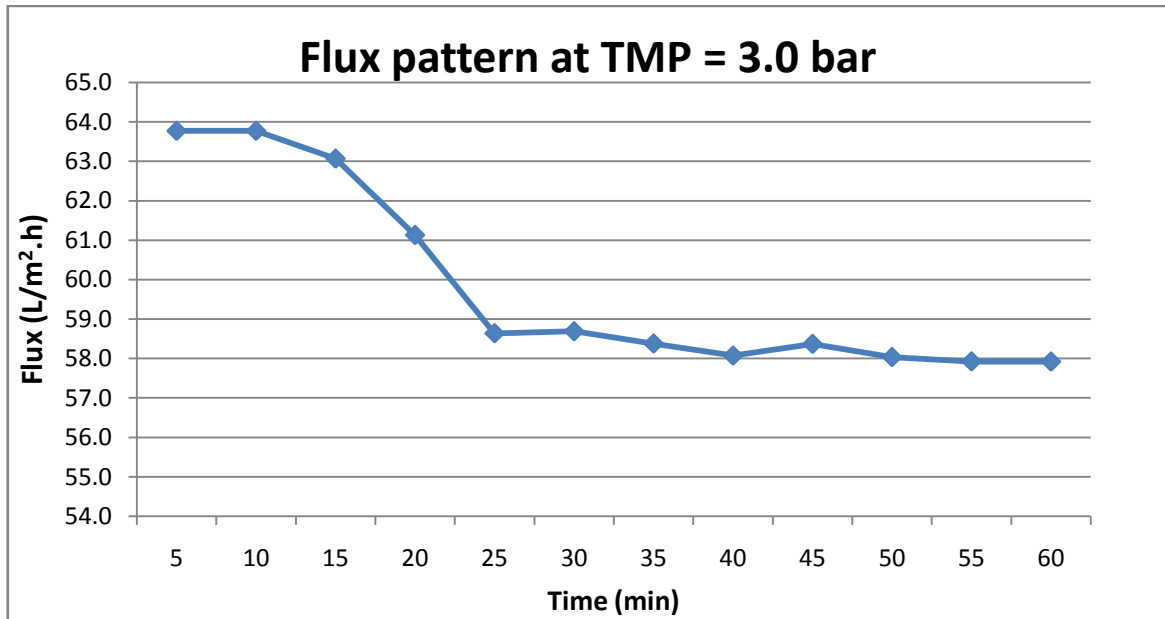
Figure 4.5: Flux pattern at TMP of 3.0 bar

Flux decline at TMP of 3.0 bars is shown at Figure 4.5. The flux pattern was obtained where the flux constantly for the first 10 minutes before gradually decreased until achieved steady state at 25 minutes. The flux was decreased for about 17.02% from 63.7783 $L/m^2.h$ to 57.9219 $L/m^2.h$ when increased in operating time. The flux was increased a little bit at 45 minutes due to the unstable flow rate of permeate that flow through the membrane and the pressure gauge reading is not constant at 3.0 bars. Compared to flux pattern at TMP of 2.5 bar from Figure 4.4, percentage of flux decreased at TMP of 3.0 bar was slightly higher when increased the value of TMP. The decrease of the flux over time is a result of fouling of the membranes. Fouling state at TMP of 3.0 bar started at first 25 minutes, compared to TMP of 2.5 bar from Figure 4.4 which started at first 35 minutes. It happened due to the increment in pressure that accelerates foulant accumulation process at membrane surface.
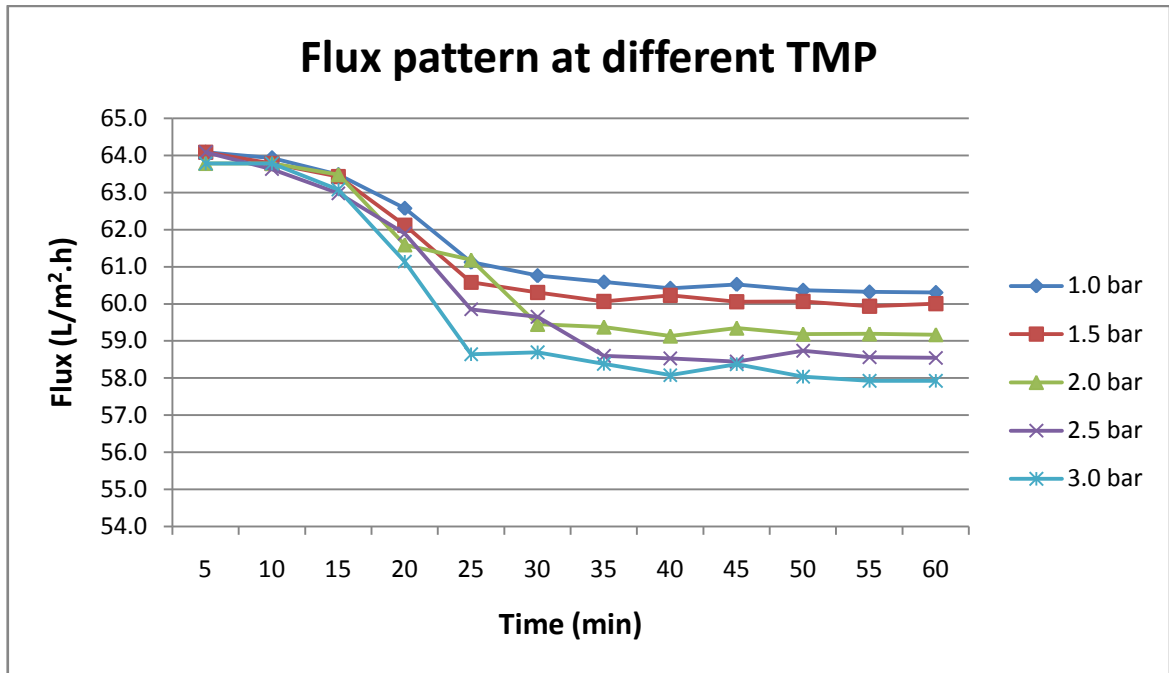
Figure 4.6: Comparison of permeate flux at different TMP

Based on Figure 4.6, the flux behavior at different TMP was shown. The effect of transmembrane pressure on the permeate flux can be observed. Increased in transmembrane pressure caused decrease of the permeate flux. Beyond a certain pressure, the decreased in permeate flux with pressure was negligible which indicates that there is an optimum pressure to obtain the maximum permeate flux. From this experiment, the highest flux was obtained at an optimum TMP of 1.0 bar with percentage of flux decline at 5.89%.

Similar results were also reported by Li et al., (2006) who obtained the optimum pressure for maximum permeate flux during the separation of cells and proteins from fermentation broth using ultrafiltration. Another findings showed that the increased in transmembrane pressure was decreased the S/N ratio in the study of effect of operating conditions on membrane fouling in treatment of pulp and paper mill wastewater by nanofiltration (Gonder et al., 2010). He added that in general, an increased in an applied transmembrane pressure could contribute to the membrane fouling which will result in increasing of osmotic pressure, and cause flux decline.

Besides that, similar phenomenon was also found by Babel and Takizawa, (2010) when treating algae-laden water using microfiltration. They found that the cake layer resistance which will result in fouling increases with the increase of TMP. No increase in resistance was found with pressure more than 30 kPa as the maximum level of compressibility was achieved.

4.3   EFFECT OF CROSS FLOW VELOCITY (CFV) ON FLUX

The flux decline was studied by performed the experiment at various cross flow velocity (CFV) which values are at 0.06, 0.10, 0.14, 0.18 and 0.22 m/s. The other variable which is transmembrane pressure (TMP) was kept constant at 1.5 bar in order to get the actual nature of dependence. The separation process was performed at 60 minutes duration at a temperature of 50 ℃.
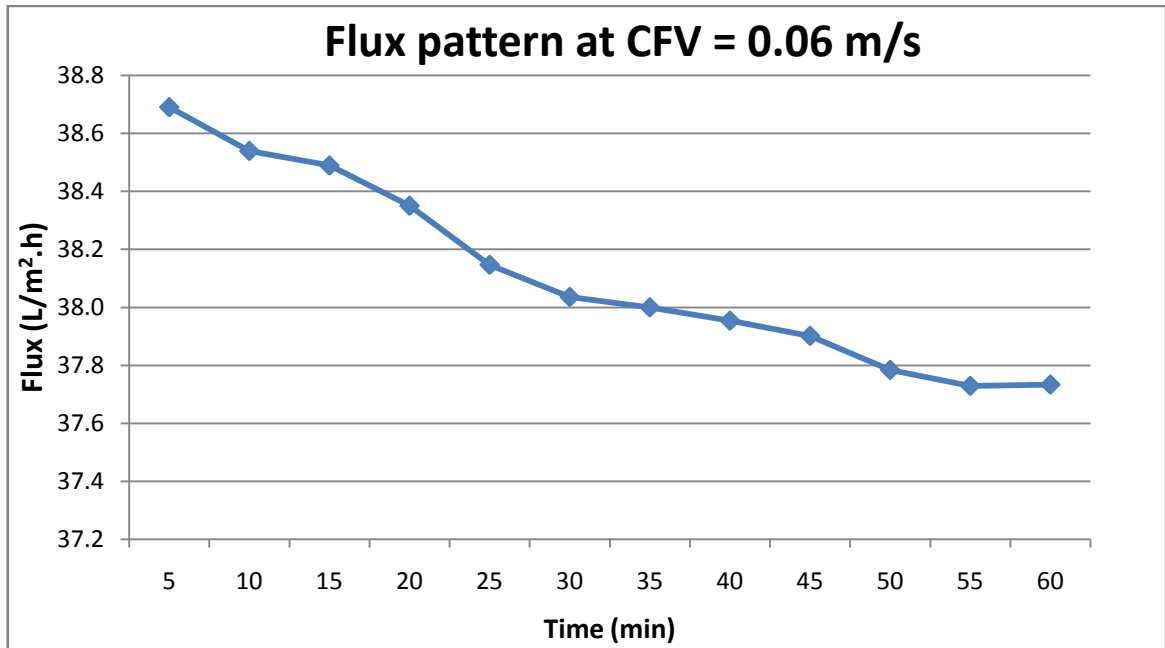
Figure 4.7: Flux pattern at CFV of 0.06 m/s

Figure 4.7 shows the flux behavior at CFV of 0.06 m/s. From the graph, the flux was constantly decreased at the first 30 minutes. The flux then decreased almost linearly before achieved steady state at last 10 minutes. This shows that the overall flux was decreased around 2.47% from 38.6902 L/m^2.h to 37.7330 L/m^2.h when the operating time increased. This is because of the performance of filter membrane was reduced due to the fouling phenomenon. Based on the graph at Figure 4.7 fouling state started at first 50 minutes due to the accumulation of foulant on membrane surface.
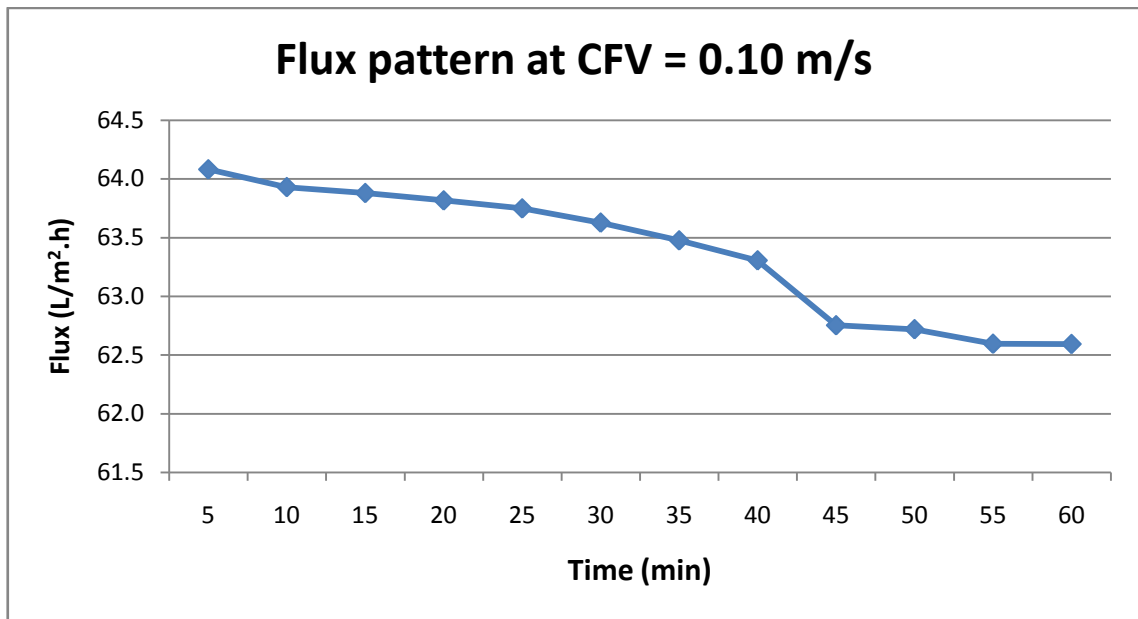
Figure 4.8: Flux pattern at CFV of 0.10 m/s

The change in permeate flux over time at CFV of 0.10 m/s was shown in Figure 4.8. The plotted pattern shows that the permeate flux was constantly decreased at the first 35 minutes and then gradually decrease until it reaches the steady state at last 10 minutes. The flux was decreased to 2.32% from 64.0806 L/m^2.h to 62.5945 L/m^2.h when the operating time increased. This shows the flux decrease happen due to the formation of cake layer on the membrane surface proportional to the operating time. Flux value at CFV of 0.10 m/s was higher compared to flux value at CFV of 0.06 m/s at Figure 4.7 due to the turbulence flow that created by high cross flow velocity. Turbulence flow scrubbed the foulant on membrane surface, hence decreased foulant accumulation on membrane surface that lead to high permeate flux.
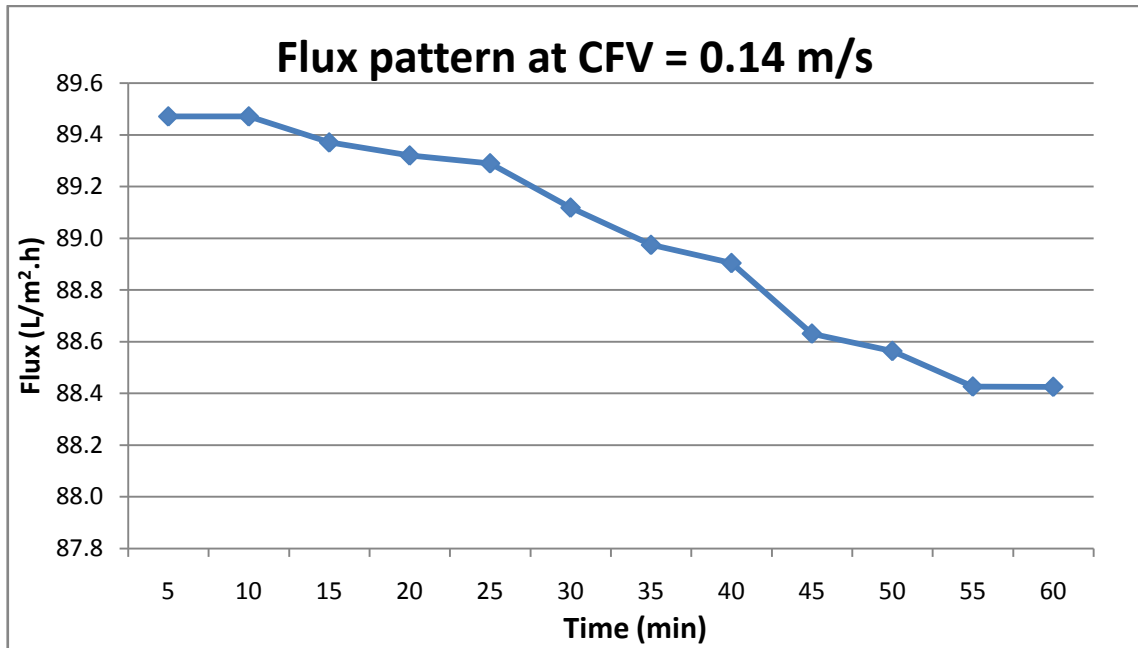
Figure 4.9: Flux pattern at CFV of 0.14 m/s

Behavior on the permeate flux at TMP of 0.14 m/s is shown in Figure 4.9. The plotted pattern shows that the permeate flux was constant for the first 10 minutes and slowly decreased till 25 minutes. Later on, the permeate flux was decreased rapidly till the last 15 minutes before it reaches the steady state condition at last 5 minutes. This shows that the flux was decreased to 1.17% from 89.4710 $L/m^2.h$ to 88.4257 $L/m^2.h$ when the operating time is increased. This is because the flow rate of the feed through the membrane was unstable and also due to the leaking on the membrane fitting through the permeate line. Flux value at CFV of 0.14 m/s was higher compared to flux value at CFV of 0.10 m/s at Figure 4.8 due to the turbulence flow that created by high cross flow velocity. Turbulence flow scrubbed the foulant on membrane surface, hence decreased foulant accumulation on membrane surface that lead to high permeate flux.
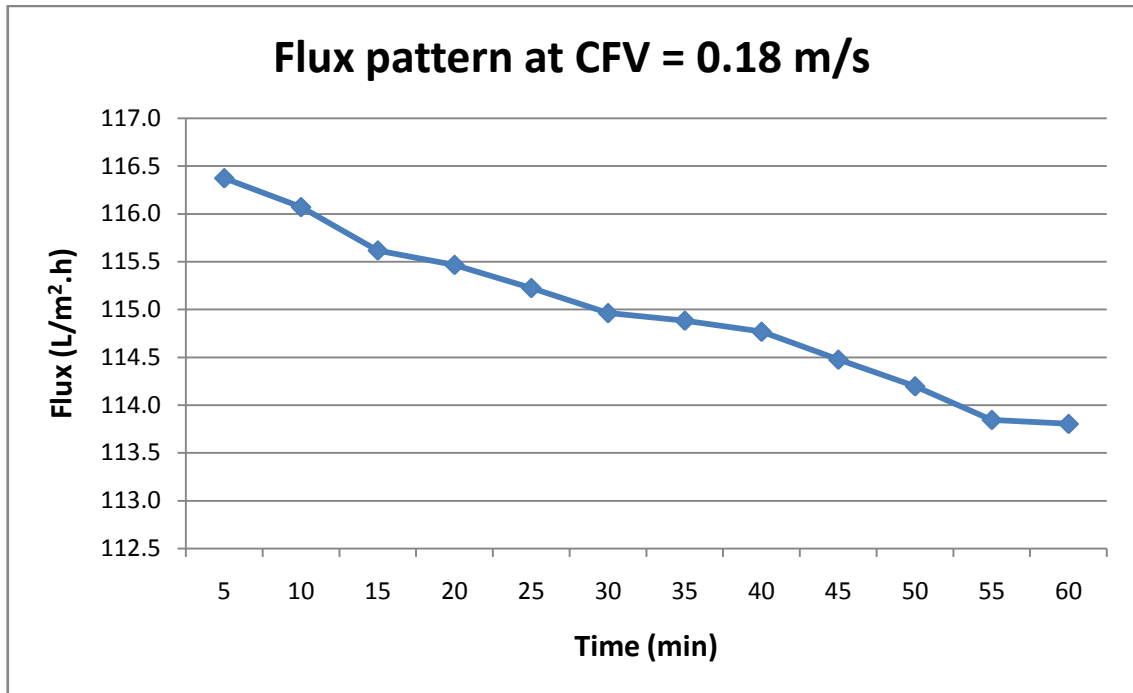
Figure 4.10: Flux pattern at CFV of 0.18 m/s

Flux behavior at CFV of 0.18 m/s is shown at Figure 4.10. The flux pattern was obtained where the flux decreased gradually before decreased linearly until achieved steady state at last 5 minutes. The flux was decreased for about 2.21% from 116.3728 L/m^2.h to 113.8035 L/m^2.h when increased in operating time. Flux value at CFV of 0.18 m/s was higher compared to flux value at CFV of 0.14 m/s at Figure 4.9 due to the turbulence flow that created by high cross flow velocity. Turbulence flow scrubbed the foulant on membrane surface, hence decreased foulant accumulation on membrane surface that lead to high permeate flux.
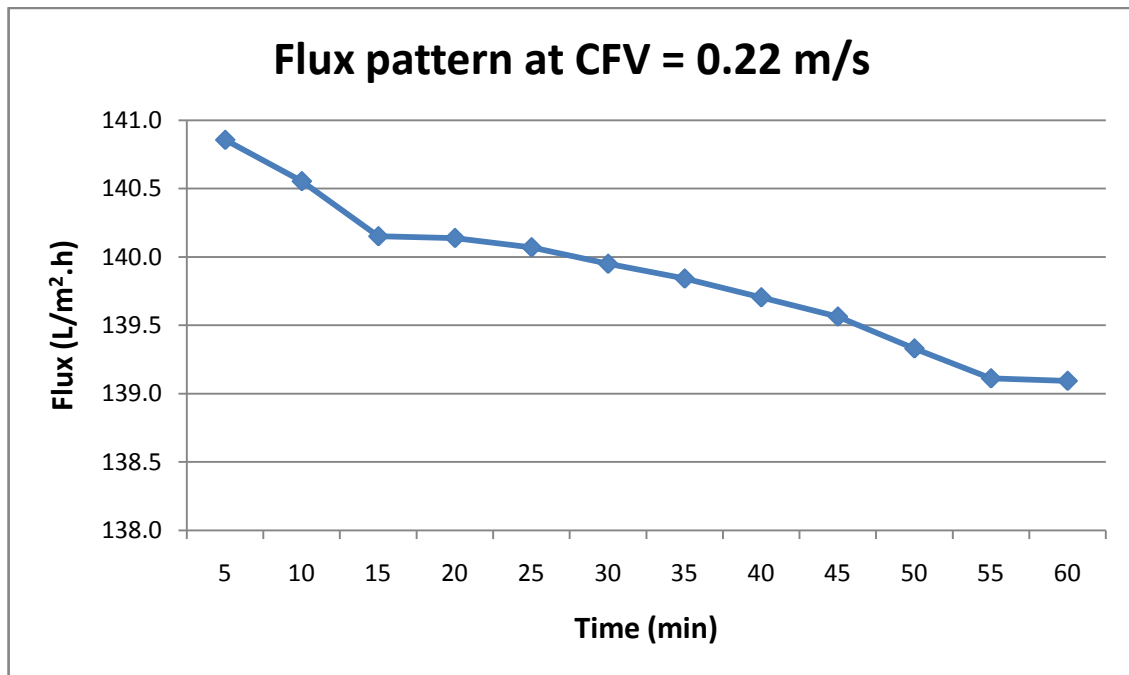
Figure 4.11: Flux pattern at CFV of 0.22 m/s

Figure 4.11 shows the flux decline at CFV of 0.22 m/s. The plotted pattern shows that the permeate flux was decreased rapidly at the first 15 minutes and then decrease gradually until it reaches the steady state at last 5 minutes. The flux was decreased to 1.25% from 140.8564 L/m^2.h to 139.0932 L/m^2.h when the operating time increased. The rapid decrease in flux shows that the membrane has fouled at the earlier stage due to the cake formation on the membrane surface. Flux value at CFV of 0.22 m/s was higher compared to flux value at CFV of 0.18 m/s at Figure 4.10 due to the turbulence flow that created by high cross flow velocity. Turbulence flow scrubbed the foulant on membrane surface, hence decreased foulant accumulation on membrane surface that lead to high permeate flux.
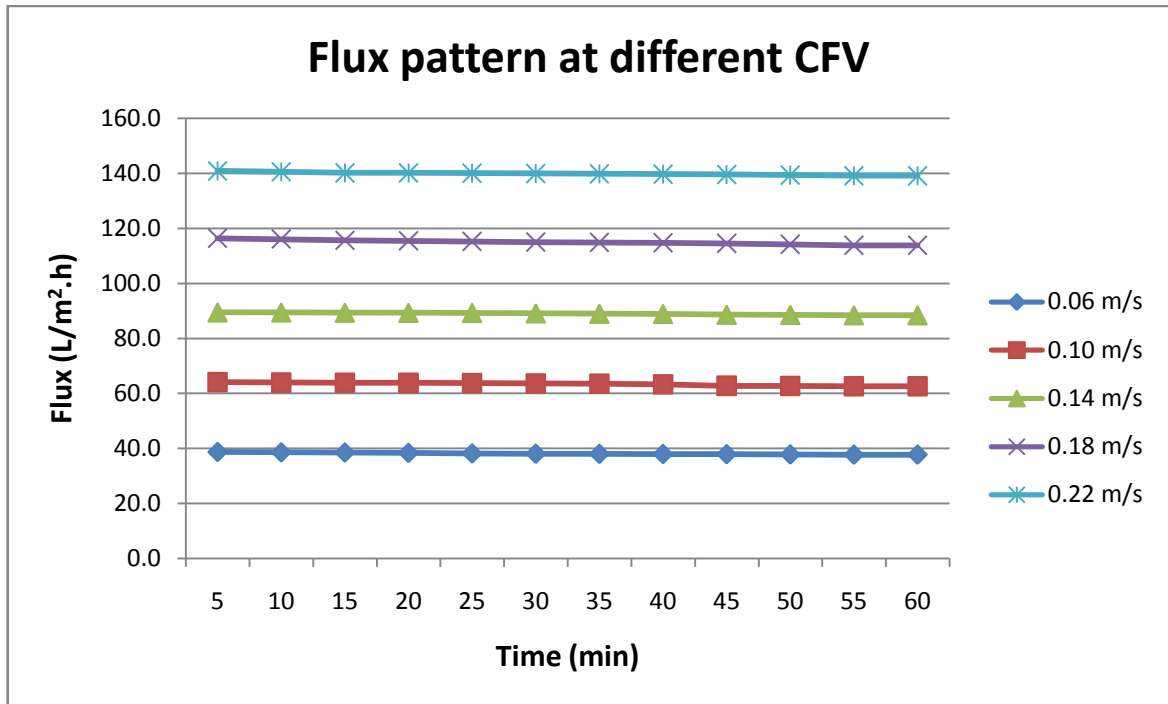
Figure 4.12: Comparison of permeate flux at different CFV

Based on Figure 4.12, the effect of cross flow velocity on the permeate flux can be observed. It is evident that an increase of cross-flow velocity caused a higher permeate flux. The decrease in permeate flux over time is a result of fouling of the membranes. Increasing the cross-flow velocity also resulted in an increase of the permeate flow rate linearly (Choi et al., 2005). From this experiment, it was found that the highest flux declined was obtained at CFV of 0.06 m/s with percentage of flux decline at 2.47% from 38.6902 L/m^2.h to 37.7330 L/m^2.h. While, the highest flux obtained at 0.22 m/s around 140.5542 L/m^2.h.

This result are in agreement with the findings of Zhong et al., (2007) who reported that the hydrodynamic forces acting on a single particle shows CFV has an important effect on the deposition of titanium salicilate-1 particles on ceramic membrane during ultrafiltration. However, after particles have deposited, increasing CFV will not resuspend them due to the strong and dense cake layer formation.

.

4.4 OPTIMIZATION OF SEPARATION OF CELLULOSE RECOVERY USING RESPONSE SURFACE METHODOLOGY

The main objective of the response surface methodology (RSM) is to determine the optimum operating conditions for the system and also to optimize the response based on the factors investigated (Idris et al., 2006). In this study, parameter of transmembrane pressure (TMP) and cross flow velocity (CFV) were selected for RSM and central composite design (CCD) was applied to identify the optimum TMP and CFV in order to maximize the permeate flux.

The response surface design developed is based on central composite design (CCD) whereby the factorial portion is a full factorial design with all combinations of the factors at two levels (high, +1 and low, −1 levels), the centre points (coded level 0), which is the midpoint between the high and low levels, is repeated five times, the axial or star points for which all but one factor is set at 1 and the one factor is set at the outer value corresponding to an α value of 2. The experimental plan generated using the Design Expert Version 6.0 software is shown in Table 4.1. The design involves 13 experimental runs and the response variables measured was the flux.

Table 4.1: Design layout and experimental results

| Standard | Run | Block | Factors | | Response |
			CFV (m/s)	TMP (bar)	Flux (L/m^2.h)
8	1	Block 1	0.14	2.50	88.244
4	2	Block 1	0.18	2.00	110.224
12	3	Block 1	0.14	1.50	88.941
9	4	Block 1	0.14	1.50	89.471
13	5	Block 1	0.14	1.50	87.765
11	6	Block 1	0.14	1.50	89.035
10	7	Block 1	0.14	1.50	90.134
5	8	Block 1	0.06	1.50	38.539
3	9	Block 1	0.10	2.00	63.778
1	10	Block 1	0.10	1.00	63.930
2	11	Block 1	0.18	1.00	116.655
7	12	Block 1	0.14	0.50	90.278
6	13	Block 1	0.22	1.50	140.554

The levels of flux at each experimental point using are given in Table 4.1. Table 4.1 showed that Standard order no. 6 which was run no. 13 gave the highest permeate flux with 140.554 L/m2.h. The operating parameter of Standard no. 6 was 1.50 bar and 0.22 m/s. The lowest permeate flux was 38.539 L/m2.h which was detected at Standard order no. 5 with the operating parameter were 1.50 bar and 0.06 m/s.

The permeate flux results were input into the Design Expert software for further analysis. Examination of the Fit Summary output revealed that the quadratic model is statistically significant for the flux rate. Therefore, this model was used to represent the responses for further analysis.

4.4.1 ANOVA Analysis

Table 4.2: ANOVA table (partial sum of square) for quadratic model (response flux)

Source	Sum of Squares	DF	Mean Square	F Value	Prob > F	
Model	7680.2506	3	2560.0835	2547.7797	< 0.0001	**significant**
A	7660.9392	1	7660.9392	7624.1205	< 0.0001	
B	9.4521	1	9.4521	9.4066	0.0134	
AB	9.8593	1	9.8593	9.8119	0.0121	
Residual	9.0435	9	1.0048			
Lack of Fit	6.0299	5	1.2060	1.6007	0.3345	**Not significant**
Pure Error	3.0136	4	0.7534			
Correlation Total	7689.2940	12				

Table 4.2 shows the *P*-values obtained were small, <0.0001 compared to a desired significance level, 0.05. This means the regression model was accurate in predicting the pattern of significance to the permeate flux.

The Model F-value of 2547.78 implies the model is significant. There is only a 0.01% chance that a "Model F-Value" this large could occur due to noise. Values of "Prob > F" less than 0.0500 indicate model terms are significant. In this case A, B, AB are significant model terms. Values greater than 0.1000 indicate the model terms are not significant model reduction may improve your model. The "Lack of Fit F-value" of 1.60 implies the Lack of Fit is not significant relative to the pure error. There is a 33.45% chance that a "Lack of Fit F-value" this large could occur due to noise.

Table 4.3: ANOVA for response surface model

Model Terms	Values
R-Squared	0.9988
Adj R-Squared	0.9984
Pred R-Squared	0.9968
Adeq Precision	181.7632

Table 4.4: Regression coefficient and P- value calculated from the model

Variable	Coefficient	P-value^a (Prob > F)
Offset	88.95	
A	25.17	< 0.0001
B	-0.99	0.0134
AB	-1.87	0.0121

＊Values of P-value less than 0.0500 indicate model terms are significant.

Table 4.2 and 4.3 show the ANOVA and regression analysis for the determination of permeate flux. The precision of a model is indicated by the determination coefficient ($R2$) and correlation coefficient (R). The determination coefficient ($R2$) implies that the sample variation of 99.88% for determination of permeate flux was attributed to the independent variables tested. The $R2$ value also indicates that only 0.12% of the total variation was not explained by the model. The value of R (correlation coefficient) closer to 1 indicates the better correlation between the experimental and predicted values.

Here, the value of R (0.9936) for Equation 4.1 indicates a close agreement between the experimental results and the theoretical values predicted by the model equation. Meanwhile, the adjusted $R2$ (coefficient of determination) was calculated to be 99.84%, indicating that a good agreement existed between the experimental and predicted values of flux. The adequate precision value, which measured the signal to

noise ratio is 181.7632, which indicates an adequate signal. A ratio greater than 4 is desirable. Thus, this model can be used to navigate to the design space.

Analysis of variance (ANOVA) was used as an appropriate to the experimental design to analyze the results. The full quadratic second-order polynomial equation was found to explain the flux by applying multiple regression analysis on the experimental data. All terms regardless of their significance were included in the equation in term of coded factor and actual factor.

The final empirical model in terms of coded factors was presented as follows:

$$Flux = 88.04 + 25.17A - 0.89B - 1.57AB \tag{4.1}$$

Where, flux is the predicted response, A is the coded value of CFV; B is the coded value of TMP and AB is the coded value for CFV times with TMP. This equation consists of 1 offset, 2 linear and 1 interactions.

In terms of actual factors the final empirical models are as follows:

$$Flux = -13.21830 + 749.41833 \, CFV + 9.21481 \, TMP - 78.49875 \, CFV*TMP \tag{4.2}$$

The coefficient values of Equation 4.1 were calculated using Design Expert Software and *P*-value of every term and the interaction are listed in Table 4.2 Based on Table 4.2, the linear term of CFV (A), linear term of TMP (B) and interaction term of CFV and TMP (AB) are significant model terms that influence the flux due to the *P*-value less than 0.05.

Figure 4.13 revealed that it has no obvious pattern and unusual structure. It also shows equal scatter above and below the *x*-axis. This implies that the model proposed is adequate and there is no reason to suspect any violation of the independence or constant variance assumption.
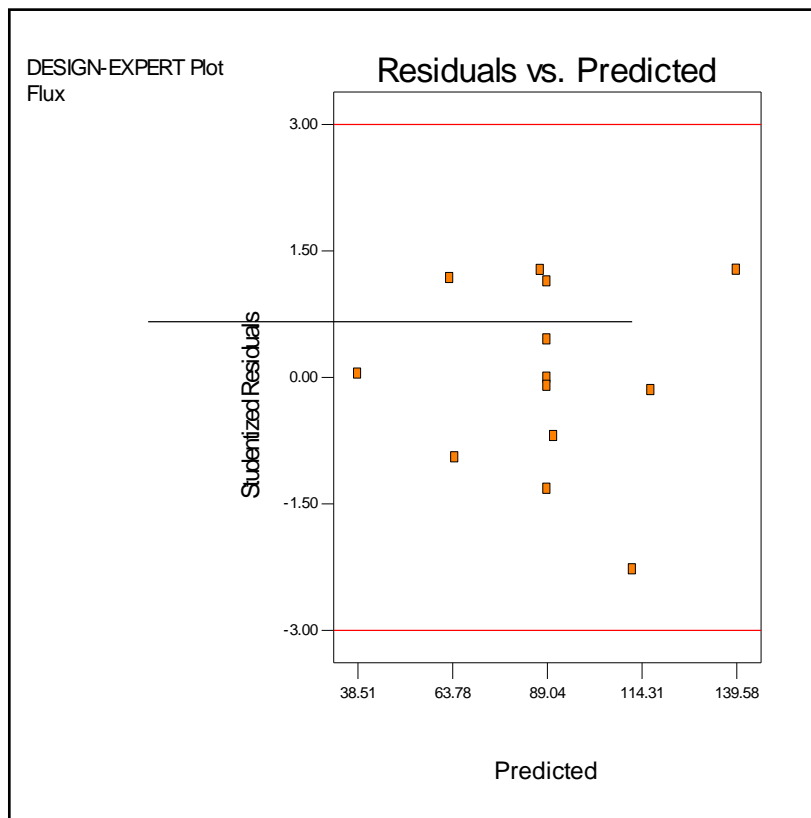
Figure 4.13: Plot of residual vs. predicted response for flux
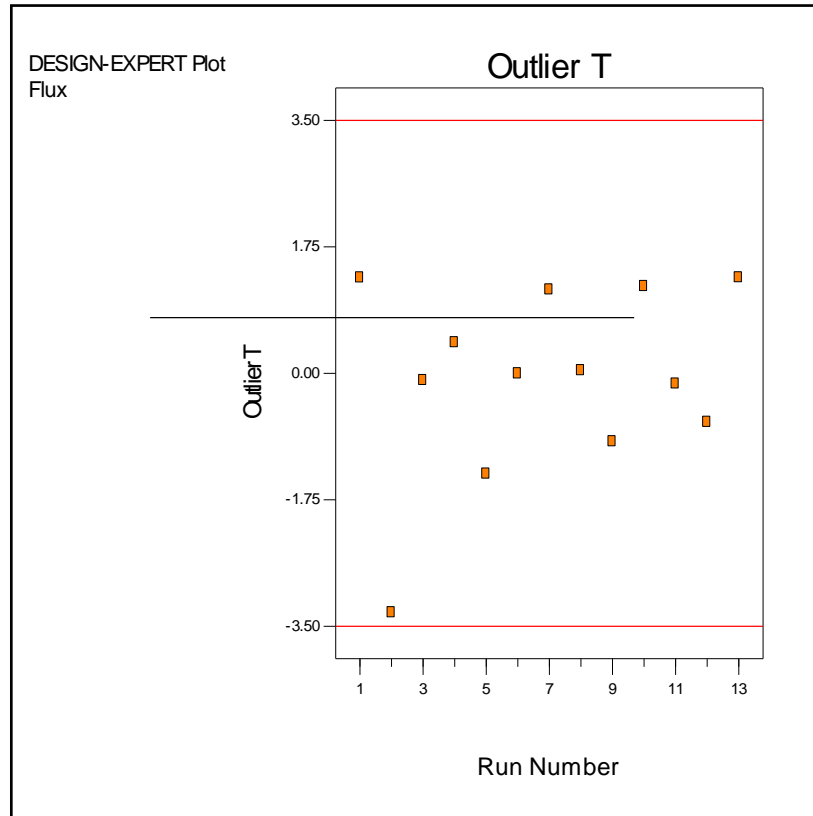
Figure 4.14: Plot of outlier T vs. run for flux

Figure 4.14 also revealed that it has no obvious pattern and unusual structure. It also shows equal scatter above and below the *x*-axis. This implies that the model proposed is adequate and there is no reason to suspect any violation of the independence or constant variance assumption.
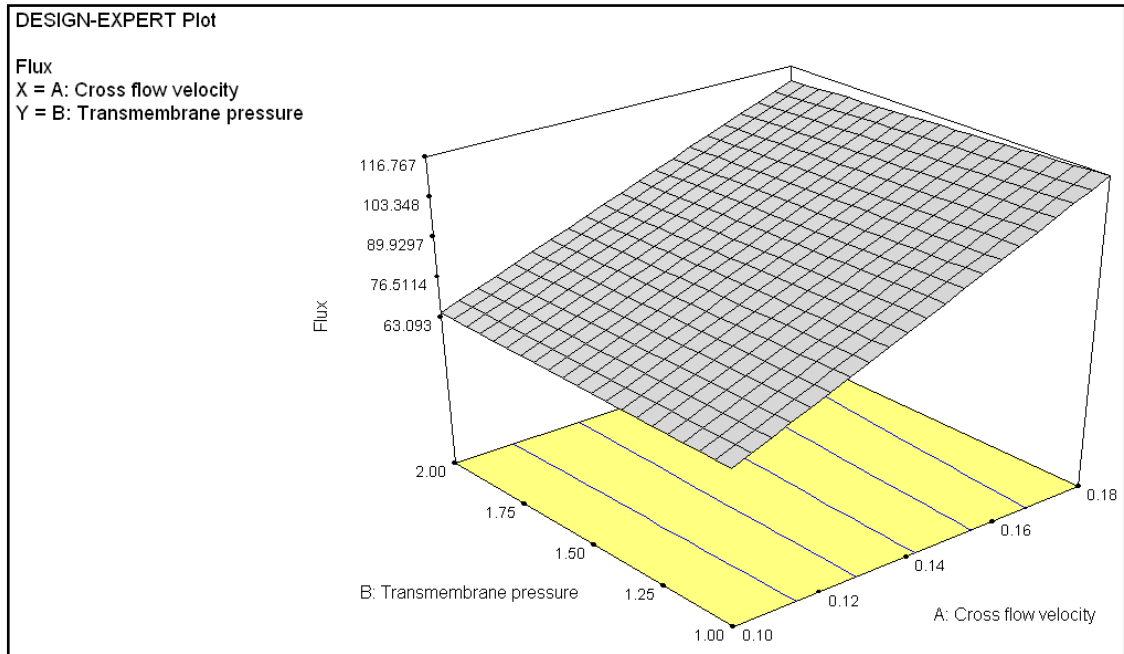
Figure 4.15: 3-D surface plot on flux for interaction of CFV (A) and TMP (B)

Figure 4.15 shows the response surface curves for the two variables in the permeate flux. The response surface representing the permeate flux was a function of one operating condition with the other one condition being at their optimal levels. Figure 4.15 revealed the operating conditions (TMP and CFV) gave the significant effect to the permeate flux. High value of CFV and TMP increased the permeate flux but the increases in TMP show a little improvement in permeate flux. Flux increases when the CFV changes from 0.10 to 0.18 m/s and TMP increases from 1.0 to 2.0 bars. The maximal permeate flux was obtained at 116.655 L/m2.h when the operating conditions was at TMP of 1.0 bar and CFV of 0.18 m/s within the duration of 15 minutes respectively.

4.4.2 Validation of Empirical Model Adequacy

Adequacy of the developed empirical models needs to be verified or validated in order to confirm the prediction accuracy. Experimental rechecking was performed using conditions that were previously used and combined with the additional experiments. Table 4.5 shows the results of operating conditions with experimental design in confirmation run. The obtained actual values and its associated predicted values from the selected experiments were compared for further residual and percentage error of analysis.

Table 4.5: Results of operating conditions with experimental design in confirmation run

No	CFV (m/s)	TMP (bar)	Predicted Flux (L/m^2.h)	Actual Flux (L/m^2.h)	Residual	% Error
1	0.18	2.00	111.310	110.224	-0.00985	0.99
2	0.14	1.50	89.035	92.740	3.705	4.00
3	0.18	1.00	116.655	120.680	4.025	3.34

Residual = (Actual value – Predicted value) (4.3)

$$\% \text{ Error} = \frac{Residual}{Actial\ value}\ x\ 100\%$$ (4.3)

The percentage error between actual and predicted value of response over a selected range of operating levels are calculated based on equation 4.3 and 4.4. Results of Table 4.5 have shown that the percentage errors are ranging from 0.99% to 4.00% for permeate flux. Thus implied that the empirical model developed were considerably accurate for responding term which is permeate flux as the percentage error between the actual and the predicted values were well within the value of 10%, suggesting that the model adequacy is reasonably within the 90.0% of prediction interval.

4.5 DINITROSALICYLIC COLORIMETRIC METHOD (DNS)

Dinitrosalicylic Colorimetric Method (DNS) was used to determine glucose concentration level in filtrate samples. Standard calibration curve that need to figure out the equation of the glucose concentration was shown in Figure 4.16. From the graph, the coefficient R^2 was 0.999 and the equation was y=2.177x + 0.362; where x-axis is a glucose production and y-axis is an absorbance of the UV VIS at 540nm.
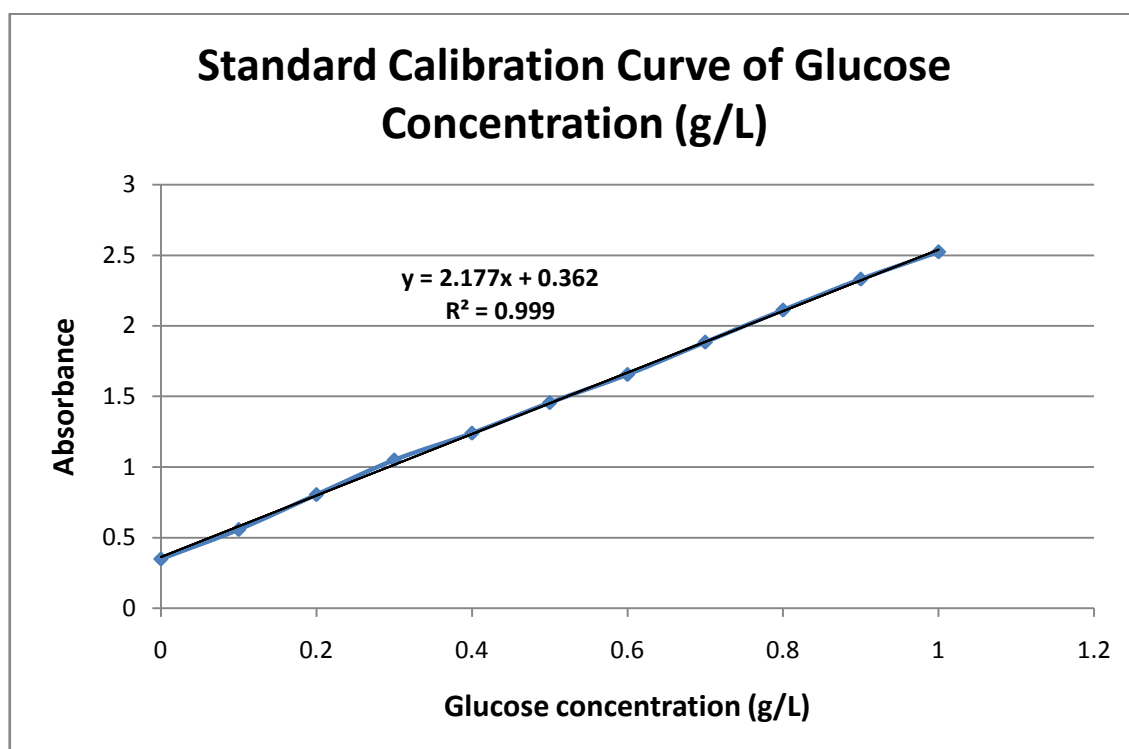
Figure 4.16: The Calibration curve of cellulose concentration

Five samples obtained were selected to test glucose content by Dinitrosalicylic Colorimetric Method (DNS). Samples were tested using UV Vis Spectrometer to determine the absorbance value. Then, absorbance values obtained from each samples were compared with standard calibration curve of glucose concentration. Results obtained as follow:

Table 4.6: Glucose concentration in samples

No.	Sample		Absorbance		Glucose Concentration (g/L)	
	CFV (m/s)	TMP (bar)	Before Filter	After Filter	Before Filter	After Filter
1	0.22	1.50	1.599	2.027	0.568	0.765
2	0.06	1.50	1.435	1.872	0.493	0.694
3	0.14	1.50	1.546	1.928	0.544	0.719
4	0.18	1.00	1.62	2.036	0.578	0.769
5	0.10	0.10	1.483	1.957	0.515	0.733

From data obtained in Table 4.6, glucose concentration in the samples after filtration is higher than glucose concentration in samples before filtration. It shows that glucose content in samples became more concentrated after filtration process by filter out suspended solid in sample solution.

Glucose content in sample no. 4 at CFV 0.18 m/s and TMP at 1.0 bars has the highest yield of concentration which is 42.28% more concentrated after filtration process. This happened due to the high permeate flux obtained from sample no. 4 which is 116.655 $L/m^2.h$. Increased in flux could reduce accumulation of flocculants on membrane surface, hence allowed more glucose to pass through the membrane filter. While, glucose content in sample no. 3 has the lowest yield of glucose concentration which is 32.26% concentrated after filtration process.

4.6   FOURIER TRANSFORM INFRARED SPECTROSCOPY (FTIR)

FTIR spectroscopy was used to study the changes of chemical structure in samples. In this study, the FTIR spectroscopy was used as a complementary technique to characterize the structure sawdust biomass after treatment with NaOH, H_2SO_4 and after enzymatic hydrolysis process. Glucose is one of the sugars that produced from enzymatic hydrolysis process. Glucose is the monosaccharide that had been hydrolyzes from polysaccharide, and enzyme was used as a catalyst in that reaction.

Figure 4.17: Comparison of sawdust biomass between before and after NaOH treatment

The bonding formation of sawdust biomass was confirmed by the FTIR spectroscopic analysis of the untreated and treated wood sawdust with NaOH solution, as shown in Figure 4.17. The FTIR spectrum of the untreated wood sawdust clearly shows the absorption bands in the region of 3826.33 cm^{-1}, 3019.79 cm^{-1} and 1700 cm^{-1} due to O-H stretching vibration, C-H stretching vibration, and C=0 stretching vibration, respectively. These absorption bands are due to hydroxyl group in cellulose, carbonyl group of acetyl ester in hemicellulose, and carbonyl aldehyde in lignin. Percentage of reflection for treated sawdust show a declination at O-H stretching vibration, C-H stretching vibration, and C=0 stretching vibration, respectively. It is because the ester carbonyl bonds in the hemicellulose and lignin were break due to the chemical treatment. All the difference happen between the untreated and treated cellulose

biomass was confirm the chemical treatment onto the sawdust (Muhammad et al., 2011).
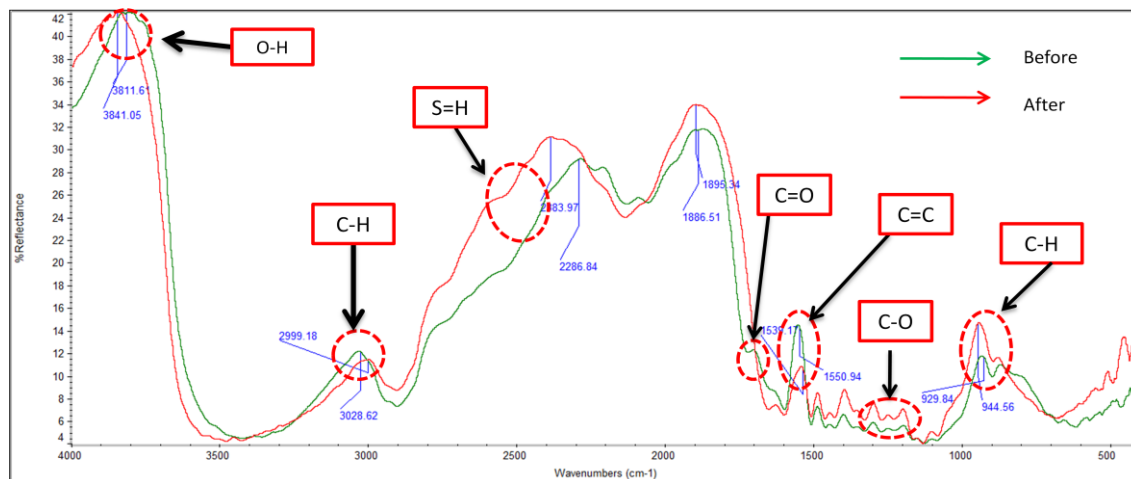
Figure 4.18: Comparison of sawdust biomass between before and after H_2SO_4 treatment

The bonding formation of sawdust biomass was confirmed by the FTIR spectroscopic analysis of the untreated and treated wood sawdust with H_2SO_4 solution, as shown in Figure 4.18. The FTIR spectrum of the untreated wood sawdust clearly shows the absorption bands in the region of 3841.05 cm^{-1}, 2999.18 cm^{-1} and 1700 cm^{-1} due to O-H stretching vibration, C-H stretching vibration, and C=0 stretching vibration, respectively. These absorption bands are due to hydroxyl group in cellulose, carbonyl group of acetyl ester in hemicellulose, and carbonyl aldehyde in lignin. Percentage of reflection for treated sawdust show a declination at O-H stretching vibration, C-H stretching vibration, and C=0 stretching vibration, respectively. It is because the ester carbonyl bonds in the hemicellulose were break due to the chemical treatment. All the difference happen between the untreated and treated cellulose biomass was confirm the chemical treatment onto the sawdust (Muhammad et al., 2011).
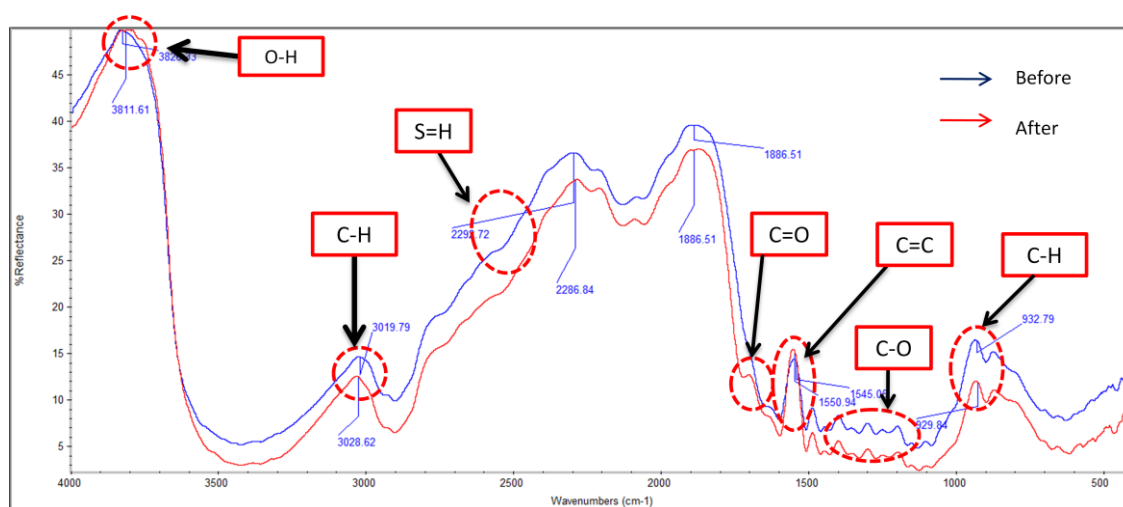
Figure 4.19: Comparison of sawdust biomass between before and after enzymatic hydrolysis

The bonding formation of sawdust biomass was confirmed by the FTIR spectroscopic analysis of the untreated and treated wood sawdust with H2SO$_4$ solution, as shown in Figure 4.19. The FTIR spectrum of the untreated wood sawdust clearly shows the absorption bands in the region of 3841.05 cm^{-1}, 2999.18 cm^{-1} and 1700 cm^{-1} due to O-H stretching vibration, C-H stretching vibration, and C=0 stretching vibration, respectively. These absorption bands are due to hydroxyl group in cellulose, carbonyl group of acetyl ester in hemicellulose, and carbonyl aldehyde in lignin. Percentage of reflection for treated sawdust show a declination at O-H stretching vibration, C-H stretching vibration, and C=0 stretching vibration, respectively. It is because the ester carbonyl bonds in the hemicellulose were break due to the chemical treatment. All the difference happen between the untreated and treated cellulose biomass was confirm the chemical treatment onto the sawdust (Muhammad et al., 2011). It shows that cellulose compound had converted to simpler monomer such as glucose.

CHAPTER 5

CONCLUSION AND RECOMMENDATION

5.1   CONCLUSION

High value of cross flow velocity (CFV) and transmembrane pressure (TMP) increased the permeate flux. The maximal permeate flux obtained was at 116.655 L/m^2.h when the operating conditions was at optimum TMP of 1.0 bar and CFV of 0.18 m/s. The combination between TMP and CFV enhance the permeate flux. Increasing the TMP causes a decline in permeate flux due to the compression of fouling layers on the membrane surface.

Effect of TMP and CFV on permeate flux were successfully been carried out throughout this research. The optimum TMP and CFV were achieved at 1.0 bar and 0.18 m/s. Membrane fouling in a cross-flow ultrafiltration unit can be minimised by increasing the cross-flow velocity and decreasing the operational transmembrane pressure. Besides, the objective of this research which to optimize the effect of TMP and CFV on permeate flux has also been achieved by using Response Surface Methodology.

5.2   RECOMMENDATION

In order to enhance the separation process, appropriate pretreatment should be done on the membrane filter before performed the filtration process. The pretreatment can be performed after each experiment. Besides, enzymatic membrane reactor was located at open area that expose to contamination risk. Hence, precaution steps need to be taken to avoid the enzymatic process was affected by contamination.

Besides that, further study could be done on mechanical machine such as pump performance and impeller design that can optimize the production and separation of glucose from cellulose hydrolysate. In addition, changing the pump used could increase the pump performance condition and pressure control that can overcome pump limitation.

Apart from used the dead end membrane, cross flow membrane can be used in the process for increasing the permeate flux. Cross flow membrane can reduce accumulation of flocculants on membrane surface by squashing out the flocculants to retentate line. Hence, it can increase membrane performance by increasing time for fouling to occur.

More over, other analysis method should be done to determine glucose content in filtrate solution such as by High Performance Liquid Chromatography (HPLC) Test. Total Organic Carbon (TOC) test could be done on filtrate to check its total organic carbon. Besides, Inductively Coupled Plasma Mass Spectrometry (ICPMS) analysis should be done on sawdust to analyze hazardous content such as sulfur.

REFERENCES

Affleck, R. P. 2000. *Recovery of Xylitol from Fermentation of Model Hemicelluloses Hydrolysates Using Membrane Technology*. (Master"s Thesis, Virginia Polytechnic Institute and State University, 2000). Retrieved from http://scholar.lib.vt.edu/theses/available/etd-01102001-121200/unrestricted/ turninetdII.pdf.

Ahmad, A. L., Ismail, S. and Bhatia, S. 2005. Membrane treatment for palm oil mill effluent: effect of transmembrane pressure and cross flow velocity. *Desalination*, **179**: 245-255

Ahmad, A. L., Ibrahim, N. and Bowen, W. R. 2002. Automated electrophoretic membrane cleaning for dead-end microfiltration and ultrafiltration. *Separation and Purification Technology*, **29**: 105-112.

Alriols, M. G., Garcia, A., Llano-ponte, R. and Labidi, J. 2010. Combined organosolv and ultrafiltration lignocellulosic biorefinery process. *Chemical Engineering Journal*, **157**: 113-120.

Babel, S. and Takizawa, S. 2010. Microfiltration membrane fouling and cake behavior during algal filtration. *Desalination*, **261**: 46-51.

Balakrishnan, M., Dua, M., Bhagat, J.J. 2000. Effect of operating parameters on sugarcane juice ultrafiltration: results of a field experience. *Separation and Purification Technology*, **19**: 209–220.

Batzias, F. A. and Sidiras, D. K. 2007. Simulation of dye adsorption by beech sawdust as affected by pH. *Journal of Hazardous Material*, **141**: 668-679.

Cara, C., Ruiz, E., Oliva, J. M., Saez, F. and Castro, E. 2008. Conversion of olive tree biomass into fermentable sugars by dilute acid pretreatment and enzymatic saccharification. *Bioresource Technology*, **99**: 1869-1876.

Catalayud, M. C. M., Vela, M. C. B., Blanco, S. A., Garcia, J. L. and Rodriguez, E. B. 2010. Analysis and optimization of the influence of operating conditions in the ultrafiltration of macromolecules using a response surface methodological approach. *Chemical Engineering Journal,* **156**: 337-346.

Choi, H., Zhang, K., Dionysiou, D. D., Oerther, D. B. and Sorial, G. A. 2005. Influence of cross-flow velocity on membrane performance during filtration of biological suspension. *Journal of Membrane Science,* **248**: 189-199.

Duarte, G. V., Ramarao, B. V. and Amidon, T. E. 2010. Polymer induced flocculation and separation of particulates from extracts of lignocellulosic materials. *Bioresource Technology*, **101**: 8526-8534.

Faria, L. F. F., Pereira, J. N. and Nobrega, R. 2002. Xylitol production from D-xylose in a membrane bioreactor. *Desalination,* **149**: 231-236.

Gonder, Z.B., Arayici S. and Barlas H. 2010. Advanced Treatment of Pulp and Paper Mill Wastewater by Nanofiltration Process: Effects of Operating Conditions on Membrane Fouling, *Separation and Purification Technology,* doi:10.1016/j.seppur.2010.10.018.

Guo, G., Chen, W., Men, L. and Hwang, W. 2008. Characterization of dilute acid pretreatment of silver grass for ethanol production. *Bioresource Technology,* **99**: 6046-6053.

Gyura, J., Seres, Z. and Eszterle, M. 2005. Influence of operating parameters on separation of green syrup colored matter from sugar beet by ultra- and nanofiltration. *Journal of Food Engineering,* **66**: 89-96.

Hashino, M., Katagiri, T., Kubota, N., Ohmukai, Y., Maruyama, T. and Matsuyama, H. 2010. Effect of membrane surface morphology on membrane fouling with sodium alginate. *Journal of Membrane Science.* doi:10.1016/j.memsci.2010.10.014

Hendriks, A. T. W. M. and Zeeman, G. 2009. Pretreatments to enhance the digestibility of lignocellulosic biomass. *Bioresource Technology*, **100**: 10-18.

Hu, G., Heitmann, J. A. and Rojas, O. J. 2008. Feedstock pretreatment strategies for producing ethanol from wood, bark, and forest residues. *Bioresources,* **3**: 270-294.

Huang, H. J., Ramaswamy, Shri., Tschirner, U. W. and Ramarao, B. V. 2008. A review of separation technologies in current and future biorefineries. *Separation and Purification Technology*, **62**: 1-21.

Hui, T.T, Keat, T.L, Abdul, R.M. 2010. Pretreatment of lignocellulosic palm biomass using a solvent-ionic liquid [BMIM]Cl for glucose recovery: An optimisation study using response surface Methodology. *Carbohydrate Polymers,* **83***:1862–1868*

Hwang, K. J. and Sz, P. Y. 2009 Filtration characteristics and membrane fouling in cross- flow microfiltration of BSA/dextran binary Suspension. *Journal of Membrane Science,* **347**: 75-82.

Idris, A., Kormin, F. and Noordin, M. Y. 2006. Application of response surface methodology in describing the performance of thin film composite membrane. *Separation and Purification Technology*, **49**: 271-280.

James, P. S., H.K. Shon, Saravanamuth, V., Huu H. N, and Hung N. 2006. Productivity enhancement in a cross-flow ultrafiltration membrane system through automated de-clogging operations. *Journal of Membrane Science,* **280**: 82–88.

Kumar, P., Barret, D. M., Delwiche, M. J. and Stroeve, Pieter. 2009. Methods for Pretreatment of Lignocellulosic Biomass for Efficient Hydrolysis and Biofuel Production. *Industrial. Engineering Chemical Resources*, **48**: 3713-3729.

Kumar, S., Singh, N. and Prasad, R. 2010. Anhydrous ethanol: A renewable source of energy. *Renewable and Sustainable Energy Reviews.* **14**: 1830-1844.

Lee, J. M., Shi, J., Venditti, R. A. and Jameel, H. 2009. Autohydrolysis pretreatment of Coastal Bermuda grass for increased enzyme hydrolysis. *Bioresource Technology*, *100*: 6434-6441.

Lei, W., Xudong, W., Ken-ichi, F. 2008. Effects of operational conditions on ultrafiltration membrane fouling. *D esalination* **229** :181–191

Li, Y., Shahbazi, A. and Kadzere, C. T. 2006. Separation of cells and proteins from fermentation broth using ultrafiltration. *Journal of Food Engineering,* **75**: 574-580.

Liang, Y., Wang, Z., Ye, X., Li, W., Xi, X., Yang, L., Wang, X., Zhang, J., Liu, Y. and Cai, Z. (2010). Study on the control of pore sizes of membranes using chemical methods: Part III. The performance of carbonates and bicarbonates in the membrane-making process by the chemical reaction. *Desalination*, doi:10.1016/j.desal.2010.09.004

Lin, S. H., Hung, C. L. and Juang, R. S. 2008. Effect of operating parameters on the separation of proteins in aqueous solutions by dead end ultrafiltration. *Desalination,* **234**: 116-125.

Madaeni, S. S. and Samieirad, S. 2010. Chemical cleaning of reverse osmosis membrane fouled by wastewater. *Desalination*, **257**: 80-86.

Mohammad, A. L. M. 2008. Recovery of hemicelluloses from wood hydrolysates by membrane filtration. (Master‟s Thesis, Lappeenranta University of Technology, 2000).

Muhammad A. M. M. I., Sinin H., Muhammad R. R., Muhammad S. I. 2011 Treated Tropical Wood Sawdust-Polypropylene Polymer Composite: Mechanical and Morphological Study, *Journal of Biomaterials and Nanobiotechnology*, 2011, 2, 435-444.

Mosier, N., Wyman, C., Dale, B., Elander, R., Lee, Y. Y., Holtzapple, M. and Ladisch, M. 2005. Features of promising technologies for pretreatment of lignocellulosic biomass. *Bioresource Technology*, **96**: 673-686.

Nazim, C., Hans, W., Makram, T. S., Brian E. W., Vincent, U. And Jacques, M. 1997. Effectiveness of the membrane bioreactor in the biodegradation of high molecular weight compounds. PII: S0043-1354(97)00350-3

Puro, L., Kallioinen, M., Manttari, M., Natarajan, G., Cameron, D. C. and Nystrom, M. 2010. Performance of RC and PES ultrafiltration membranes in filtration of pulp mill process waters. Desalination, doi:10.1016/j.desal.2010.06.034

Sakinah, A. M. M., Ismail, A. F., Illyas, R. M. and Hassan, O. 2007. Fouling characteristics and autopsy of a PES ultrafiltration membrane in cyclodextrins separation. *Desalination,* **207**: 227-242.

Sakinah, A. M. M., Ismail, A. F., Illias, R. M., Zularisam, A. W., Hassan, O. and Matsuura, T. 2008. Cyclodextrin production in hollow fiber membrane reactor system: Effect of substrate preparation. *Separation and Purification Technology*, **63**: 163-171.

Sun, Y. and Cheng, J. 2002. Hydrolysis of lignocellulosic materials for ethanol production: a review. *Bioresource Technology*, **83**: 1-11.

Sun, Y. and Cheng, J. J. 2005. Dilute acid pretreatment of rye straw and bermudagrass for ethanol production. *Bioresource Technology*, **96**: 1599-1606.

Thomassen, J. K., Faraday, D. B. F., Underwood, B. O. and Cleaver, J. A. S. 2005. The effect of varying transmembrane pressure and cross flow velocity on the microfiltration fouling of a model beer. *Separation and Purification Technology*, **41**: 91-100.

Wang, Z., Keshwani, D. R., Redding, A. P. and Cheng, J. J. 2010. Sodium hydroxide pretreatment and enzymatic hydrolysis of coastal Bermuda grass. *Bioresource Technology*, *101*: 3583-3585.

Wikramasinghe, S. R. and Grzenia, D. L. 2008. Adsorptive membranes and resins for acetic acid removal from biomass hydrolysates. *Desalination*, **234**: 144-151.

Zhong, Z., Xing, W., Liu, X., Jin, W. and Xu, N. 2007. Fouling and regeneration of ceramic membranes used in recovering titanium silicalite-1 catalysts. *Journal of Membrane Science*, **301**: 67-75.

Zhu, J. Y. and Pan, X. J. 2010. Woody biomass pretreatment for cellulosic ethanol production: Technology and energy consumption evaluation. *Bioresource Technology*, **101**: 4992-5002.

APPENDIX A

Preparation of Alkali and Acid solutions

A) 0.1M Sodium Hydroxide (NaOH)

$$n = \frac{MV}{1000}$$

$$\frac{m}{MW} = \frac{MV}{1000}$$

where, n = mol

     m = mass of NaOH needed

     M = molarity @ concentration of NaOH = 0.1M

     V = volume of solvent (H20), mL = 100,000 mL

     MW = molecular weight of NaOH, g/mol = 40 g/mol

Thus, 0.1M NaOH was prepared as follow:

$$\frac{m}{MW} = \frac{MV}{1000}$$

     m = ((0.1M) (100,000mL)/1000) x 40 g/mol

       = **400 g of NaOH (solid)** needed to be diluting with 100 L distilled water to

          obtained 0.1M NaOH.

B) 0.04M Sulfuric Acid (H_2SO_4)

$$M = \frac{SG \; x \; purity \; x \; 1000}{MW}$$

where, M = molarity @ concentration of stock H_2SO_4

SG = specific gravity of H2SO4 = 1.84

purity = percentage of stock H2SO4 = 96% = 0.96

MW = molecular weight H_2SO_4, g/mol = 98.08 g/mol

Molarity of H2SO4 needed from stock solution is as follow:

$$M = \frac{SG \; x \; purity \; x \; 1000}{MW} = \frac{1.84 \; x \; 1.96 \; x \; 1000}{98.08 \; g/mol}$$

$$= 18.02 \; M$$

Thus, using equation: $\qquad M_1V_1 = M_2V_2$

$$(0.04M)(100L) = (18.02M) \; V_2$$

$$V_2 = 0.22 \; L$$

$$= \textbf{220 mL stock } \mathbf{H_2SO_4} \text{ is needed to be dilute}$$

with 100 L distilled water to obtained 0.04M

H_2SO_4.

APPENDIX B

Calculation of permeate flux during separation process

Permeate flux was being calculated using following equation:

Permeate Flux, J

$$= \frac{Permeate\ volume}{membrane\ Area\ x\ time}\ (Lm^{-2}h^{-1})\ \ or \qquad J = \frac{Q}{A}$$

where, J = permeate flux, L/m^2.h

Q = permeate flow rate, mL/min

A = effective membrane area, m^2 = 0.0397 m^2

Permeate flux at constant transmembrane pressure (TMP=1.5 bar) at different values of cross flow velocity (CFV).

| Cross Flow Velocity, CFV | | | 0.06 m/s | |
| Transmembrane Pressure, TMP | | | 1.5 bar | |
Time (min)	Volume, V1 (mL)	Volume, V2 (mL)	Volume, Av (mL)	Flux (L/m2.h)
5	128	128	128	38.6902
10	255	255	255	38.5390
15	380	381	382	38.4887
20	500	515	508	38.3501
25	631	635	631	38.1461
30	749	765	755	38.0353
35	863	897	880	37.9993
40	982	1025	1005	37.9534
45	1126	1127	1129	37.9009
50	1221	1279	1250	37.7834
55	1341	1405	1373	37.7284
60	1537	1455	1498	37.7330

| Cross Flow Velocity, CFV | | | 0.10 m/s | |
| Transmembrane Pressure, TMP | | | 1.5 bar | |
Time (min)	Volume, V1 (mL)	Volume, V2 (mL)	Volume, Av (mL)	Flux (L/m2.h)
5	214	210	212	64.0806
10	431	415	423	63.9295
15	641	627	634	63.8791
20	857	832	845	63.8161
25	1065	1044	1055	63.7481
30	1278	1248	1263	63.6272
35	1489	1451	1470	63.4761
40	1682	1669	1676	63.3060
45	1867	1870	1869	62.7540
50	2065	2085	2075	62.7204
55	2268	2288	2278	62.5967
60	2479	2491	2485	62.5945

Cross Flow Velocity, CFV			0.14 m/s	
Transmembrane Pressure, TMP			1.5 bar	
Time (min)	Volume, V1 (mL)	Volume, V2 (mL)	Volume, Av (mL)	Flux (L/m2.h)
5	294	298	296	89.4710
10	587	597	592	89.4710
15	881	893	887	89.3703
20	1174	1190	1182	89.3199
25	1472	1482	1477	89.2897
30	1758	1780	1769	89.1184
35	2048	2073	2061	88.9745
40	2342	2364	2353	88.9043
45	2633	2645	2639	88.6314
50	2918	2942	2930	88.5642
55	3209	3227	3218	88.4268
60	3501	3520	3511	88.4257

Cross Flow Velocity, CFV			0.18 m/s	
Transmembrane Pressure, TMP			1.5 bar	
Time (min)	Volume, V1 (mL)	Volume, V2 (mL)	Volume, Av (mL)	Flux (L/m2.h)
5	388	382	385	116.3728
10	773	763	768	116.0705
15	1153	1142	1148	115.6171
20	1530	1526	1528	115.4660
25	1901	1911	1906	115.2242
30	2274	2290	2282	114.9622
35	2663	2668	2661	114.8831
40	3027	3048	3038	114.7670
45	3391	3426	3409	114.4752
50	3753	3803	3778	114.1965
55	4104	4182	4143	113.8447
60	4474	4562	4518	113.8035

Cross Flow Velocity, CFV			0.22 m/s	
Transmembrane Pressure, TMP			1.5 bar	
Time (min)	Volume, V1 (mL)	Volume, V2 (mL)	Volume, Av (mL)	Flux (L/m2.h)
5	470	462	466	140.8564
10	1097	763	930	140.5542
15	1640	1142	1391	140.1511
20	2183	1526	1855	140.1385
25	2723	1911	2317	140.0705
30	3266	2290	2778	139.9496
35	4209	2268	3239	139.8417
40	4347	3048	3698	139.7040
45	4885	3426	4156	139.5634
50	5416	3803	4610	139.3300
55	5943	4182	5063	139.1115
60	6482	4562	5522	139.0932

Permeate flux at constant cross flow velocity (CFV=0.10 m/s) at different values of transmembrane pressure (TMP).

Cross Flow Velocity, CFV			0.10 m/s	
Transmembrane Pressure, TMP			1.0 bar	
Time (min)	Volume, V1 (mL)	Volume, V2 (mL)	Volume, Av (mL)	Flux (L/m2.h)
5	214	210	212	64.0806
10	428	418	423	63.9295
15	639	621	630	63.4761
20	836	820	828	62.5693
25	1015	1007	1011	61.1184
30	1204	1208	1206	60.7557
35	1399	1407	1403	60.5829
40	1595	1603	1599	60.4156
45	1795	1809	1802	60.5206
50	1982	2012	1997	60.3627
55	2187	2203	2195	60.3160
60	2392	2396	2394	60.3023

Cross Flow Velocity, CFV			0.10 m/s	
Transmembrane Pressure, TMP			1.5 bar	
Time (min)	Volume, V1 (mL)	Volume, V2 (mL)	Volume, Av (mL)	Flux (L/m2.h)
5	212	212	212	64.0806
10	426	418	422	63.7783
15	632	627	630	63.4257
20	815	829	822	62.1159
25	996	1008	1002	60.5743
30	1182	1212	1197	60.3023
35	1273	1509	1391	60.0648
40	1585	1603	1594	60.2267
45	1775	1801	1788	60.0504
50	1961	2013	1987	60.0605
55	2134	2228	2181	59.9313
60	2340	2424	2382	60.0000

Cross Flow Velocity, CFV			0.10 m/s	
Transmembrane Pressure, TMP			2.0 bar	
Time (min)	Volume, V1 (mL)	Volume, V2 (mL)	Volume, Av (mL)	Flux (L/m2.h)
5	209	213	211	63.7783
10	428	416	422	63.7783
15	631	629	630	63.4761
20	792	838	815	61.5869
25	997	1027	1012	61.1788
30	1137	1223	1180	59.4458
35	1331	1419	1375	59.3739
40	1503	1627	1565	59.1310
45	1712	1822	1767	59.3451
50	1899	2017	1958	59.1839
55	2120	2188	2154	59.1894
60	2395	2303	2349	59.1688

Cross Flow Velocity, CFV			0.10 m/s	
Transmembrane Pressure, TMP			2.5 bar	
Time (min)	Volume, V1 (mL)	Volume, V2 (mL)	Volume, Av (mL)	Flux (L/m2.h)
5	212	212	212	64.0806
10	424	418	421	63.6272
15	621	629	625	62.9723
20	803	835	819	61.8892
25	974	1006	990	59.8489
30	1164	1204	1184	59.6474
35	1314	1400	1357	58.5966
40	1493	1605	1549	58.5264
45	1683	1797	1740	58.4383
50	1894	1992	1943	58.7305
55	2063	2199	2131	58.5574
60	2270	2378	2324	58.5390

Cross Flow Velocity, CFV			0.10 m/s	
Transmembrane Pressure, TMP			3.0 bar	
Time (min)	Volume, V1 (mL)	Volume, V2 (mL)	Volume, Av (mL)	Flux (L/m2.h)
5	210	212	211	63.7783
10	426	418	422	63.7783
15	623	629	626	63.0730
20	805	813	809	61.1335
25	937	1003	970	58.6398
30	1143	1187	1165	58.6902
35	1318	1386	1352	58.3807
40	1489	1585	1537	58.0730
45	1699	1777	1738	58.3711
50	1884	1956	1920	58.0353
55	2066	2150	2108	57.9253
60	2278	2321	2300	57.9219